CONTROL METHODS FOR POWERED ASSISTIVE DEVICES FOR INDIVIDUALS WITH MOBILITY IMPAIRMENTS: COMPENSATING FOR DISRUPTED PHYSIOLOGICAL CONTROL LOOPS

By

Kevin H. Ha

Dissertation

Submitted to the Faculty of the

Graduate School of Vanderbilt University

in partial fulfillment of the requirements

for the degree of

DOCTOR OF PHILOSOPHY

in

Mechanical Engineering

May, 2015

Nashville, Tennessee

Approved:

Michael Goldfarb, Ph.D.

Eric J. Barth, Ph.D.

Robert J. Webster, Ph.D.

Peter E. Konrad, M.D., Ph.D.

For my parents, my brother, and our past, current, and future dogs

ACKNOWLEDGMENTS

It is purely by chance that I ended up at the Center for Intelligent Mechatronics. Sometime in 2007, I had coffee with Dr. Peter Konrad, a neurosurgeon with a Ph.D. in electrical engineering, to talk about potential research opportunities. After a short talk, Dr. Konrad's message was clear; I should talk to Dr. Michael Goldfarb, because he does really cool stuff. After that, I somehow ended up joining Dr. Goldfarb's lab as a Ph.D. student. Little did he know that I knew nothing about engineering. I must first acknowledge Dr. Goldfarb for being patient and allowing me to learn over the past six years. I would also like to acknowledge Dr. Konrad for introducing me to Dr. Goldfarb, and for being a great role model as one of only a handful of neurosurgeon engineers in the country. I ended up choosing a different field of medicine, but the decision would have been much more difficult without Dr. Konrad's input and guidance.

This work would not have been possible without the help of other members of the lab. Drs. Frank Sup and Atakan Varol were always willing to provide help and guidance during my first few years in the lab. Drs. Ryan Farris and Hugo Quintero designed an excellent exoskeleton that has been essential to my work over the past few years. We have been extremely fortunate to have Clare Hartigan and Scott Hawes as clinical advisors for the project. The exoskeleton would not be what it is today without their contributions. Spencer Murray, Ben Gasser, and Andrew Ekelem have all been great teammates on the exoskeleton project, especially Spencer, with whom I shared a hotel room way too many times. Dr. Brian Lawson has been very helpful in the process of writing this dissertation by providing me with a well-written dissertation of his own from which to copy the formatting. And of course, the miracle workers of our lab, Don Truex and Jason Mitchell, were somehow always able to fix things that we (the graduate students) could not figure out.

Last but not least, I would like to acknowledge the graduate students on the fifth floor of Olin Hall for making my graduate school experience more fun than it probably should have been.

TABLE OF CONTENTS

Page

LIST OF FIGURES

Figure Page

LIST OF TABLES

Table Page

CHAPTER I

INTRODUCTION

This document summarizes the research that I have completed at the Center for Intelligent Mechatronics between August, 2008 and June, 2014. The presented work is by no means achieved on my own, but is rather a part of collective effort by a group of researchers at the center lead by Dr. Michael Goldfarb, who has made significant contributions to the field of assistive and rehabilitative robotics. My work has focused on the control of assistive devices for individuals with limb amputations and spinal cord injuries. This chapter describes the motivation behind this work, followed by a brief overview of the physiology behind the control of human movement in terms of neural science and physiological control loops.

The remaining chapters consist of published (or soon to be published) works describing the specific control methods and their implementation. Chapter II describes the use of pattern recognition of physiological signals for volitional control of powered prostheses. This manuscript was published in the *IEEE Transactions on Biomedical Engineering*. Chapter III describes the implementation of a dynamic step trigger within a finite-state control structure that improves the walking speed of a powered lower limb exoskeleton for individuals with paraplegia. This manuscript is ready to be submitted to a journal to be determined. Chapter IV describes the use of a cooperative control method for a system consisting of paralyzed muscles activated by functional electrical stimulation (FES) and powered lower limb exoskeletons for gait restoration in paraplegic individuals. This manuscript has been accepted for publication in the *IEEE Transactions on Neural Systems and Rehabilitation Engineering*.

1. Motivation

With recent advances in robotic technology, assistive devices designed to restore legged mobility for the mobility impaired have started to emerge in both research and commercial settings. Using embedded sensors, actuators, and microcontrollers, these devices are capable of performing

precise movements. However, because an assistive device must work with a human user, it must perform the movements at the appropriate moment (e.g. when the user wants it to) to ensure proper operation. Furthermore, depending on the nature of the user's impairment, many of the user's physiological control loops necessary for proper motor control are disrupted. To ensure safe operation as an assistive device, the device must compensate for the disrupted control loops in some manner.

2. Physiologic Control of Movement

The information presented in this section is obtained predominantly from various chapters in *Principles of Neural Science* by Kandel, Schwartz, and Jessell (4th edition, 2000). This section is designed to serve as a background material for the pathophysiology behind limb amputations and spinal cord injuries. I have put together Figures 1.1, 1.2, and 1.3 in order to provide a simplified description of the physiology of purposeful movement, based on my understanding of the information from *Principles of Neural Science.*

2.1 Overview

Physiologic control of purposeful movement requires continuous interactions between the sensory and motor systems. The sensory system combines various types of sensory information about the body and the environment, such as joint position, visual, vestibular, and auditory information, to form spatiotemporal images of the person's own body, as well as how it is interacting with the environment [1]. Multiple areas of the cerebral cortex, cerebellum, basal ganglia, thalamus, brain stem, and spinal cord are involved in the planning, coordination, and execution of purposeful action [2]. Some areas are involved in high-level control, such as decision making and planning of movement. Other areas are involved in low-level control, such as coordination and execution of movement.

2.2 Sensors

In the human body, sensory receptors throughout the body provide sensory information about the body and the surrounding environment. Sensory areas of the cerebral cortex use the signals from throughout the body to convert the sensory signals into cognition. For example, understanding the position and spatial orientation of lower limbs and how they are moving in space requires

sensory information from multiple sources. First, information about joint angles and how fast they are moving are sensed by muscle spindles and golgi tendon organs in skeletal muscles [3]. The sensory receptors then send the sensory information to the spinal cord via sensory fibers in the form of action potentials (described in Chapter I Section 2.4) [3]. The spinal cord relays the signals to the cerebral cortex. The brain then integrates the joint position information with the spatial orientation of the body, which is provided by the vestibular system, to form an image of the position and spatial orientation of the limbs, as well as how they are moving in space. Many other sensory systems, such as the visual system and auditory system, are also integrated and processed to form a complete internal image of the body and the surrounding environment.

2.3 Controllers

The central nervous system (CNS) carries out the function of the controller. Multiple areas of the brain and the spinal cord are involved in the planning and execution of purposeful movement based on the sensory input and the intended action (Figure 1.1) [2]. Specifically, the thalamus acts as a switchboard for incoming sensory information and relays it to the cerebral cortex. The cerebellum plays a major role in managing the timing and coordination of movement [4]. Areas of the cerebral cortex manage high-level control of movement, such as the movement planning, decision making, and making adjustments to anticipated disturbance. The brainstem and the spinal cord act as a relaying station for ascending and descending signals between the body and the brain, as almost all sensory and motor signals must go through the spinal cord and the brainstem. Low-level details and coordination of movement are carried out by spinal circuits, which are regulated by descending signals from the brain [5].

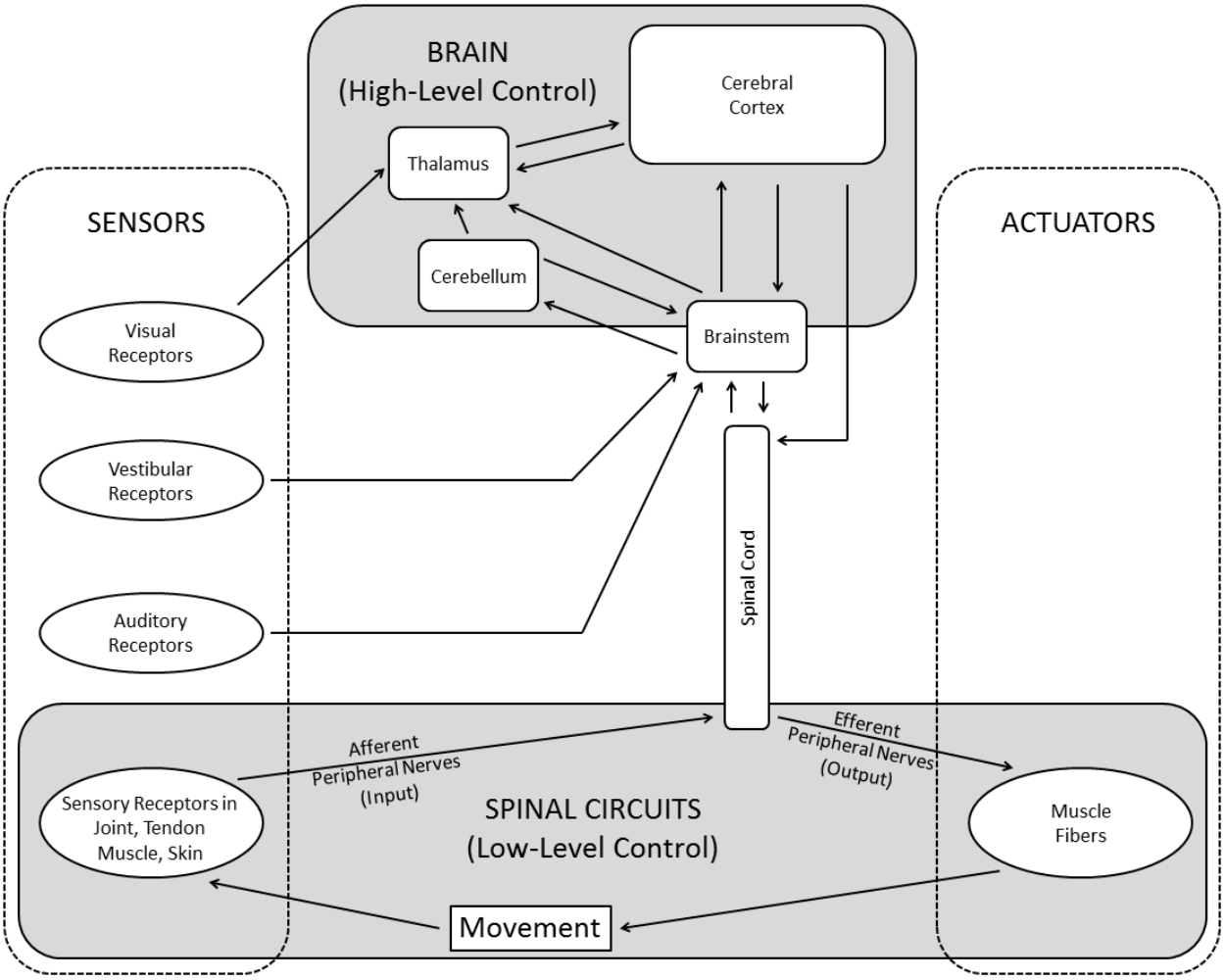

Figure 1.1. Overview of the physiologic control of purposeful movement

2.4 Transmission of Signals

An axon of a neuron is a long elongated structure that conducts nerve impulses from the cell body to another site [3]. It can be thought of as a conductive wire that transmits signals throughout the body. A signal travels down an axon in a series of changes in electric potentials across the cell membrane, called an action potential. An action potential propagates down an axon because there are voltage-gated ion channels that are activated by a nearby action potential [3].

2.5 Actuators

Actuators used for purposeful movement are skeletal muscles crossing one or more joints. When an action potential reaches a myocyte (muscle cell), calcium ions are released into the cytoplasm (intracellular space) from a specialized organelle within the myocyte. The release of calcium ions allow overlapping filaments within the muscle (actin and myosin) slide past each other, resulting in shortening of the overall length of the muscle [6]. The resulting contraction of a muscle group generates torque at the joint it crosses.

3. Physiology of Electromyography (EMG) and Functional Electrical Stimulation (FES)

This section gives a brief description of two methods that can be used to interface robotic devices with the neural control loops. The first method can be used to convey physiological motor output signals from the user to the device. The second method can be used to convey motor output signals from the device to the user.

3.1 EMG

Contraction of a muscle requires movement of charged ions throughout the muscle. Because the fibers in the muscle are activated in an asynchronous manner, the flow of charged ions results in temporal changes in electric potential across the muscle. Surface electrodes on the skin over a muscle can detect these changes in electric potential during muscle activity. This is called surface electromyography (EMG) [6]. In the case of a limb amputation, EMG can be used to detect muscle activity in the residual limb, as shown in Figure 1.2.

3.2 FES

Propagation of an action potential is mediated by voltage-gated sodium channels along the axon of a neuron [3]. Because these channels open or close based on the electric potential across the cell membrane, anything that changes the membrane potential past the activation threshold will trigger an action potential along the axon. When an external source of current is applied across peripheral nerves innervating a muscle group, the resulting action potentials can activate the innervated muscle group. This is called functional electrical stimulation (FES) [7]. FES can be used to activate paralyzed muscles of individuals with spinal cord injuries, as long as the peripheral nerves innervating the muscles are intact, as shown in Figure 1.3.

4. Effects of Limb Amputation on Control of Movement

In the case of a limb amputation, everything distal to the injury site is missing, including some portions of the sensory receptors and actuators, as shown in Figure 1.2. Most of the time, there are intact residual muscles and sensory receptors proximal to the injury, but because the activation of residual muscles does not result in joint movement, the sensory receptors no longer provide correct information. As a result, the low-level control loops are disrupted in the case of a limb amputation (Figure 1.2).

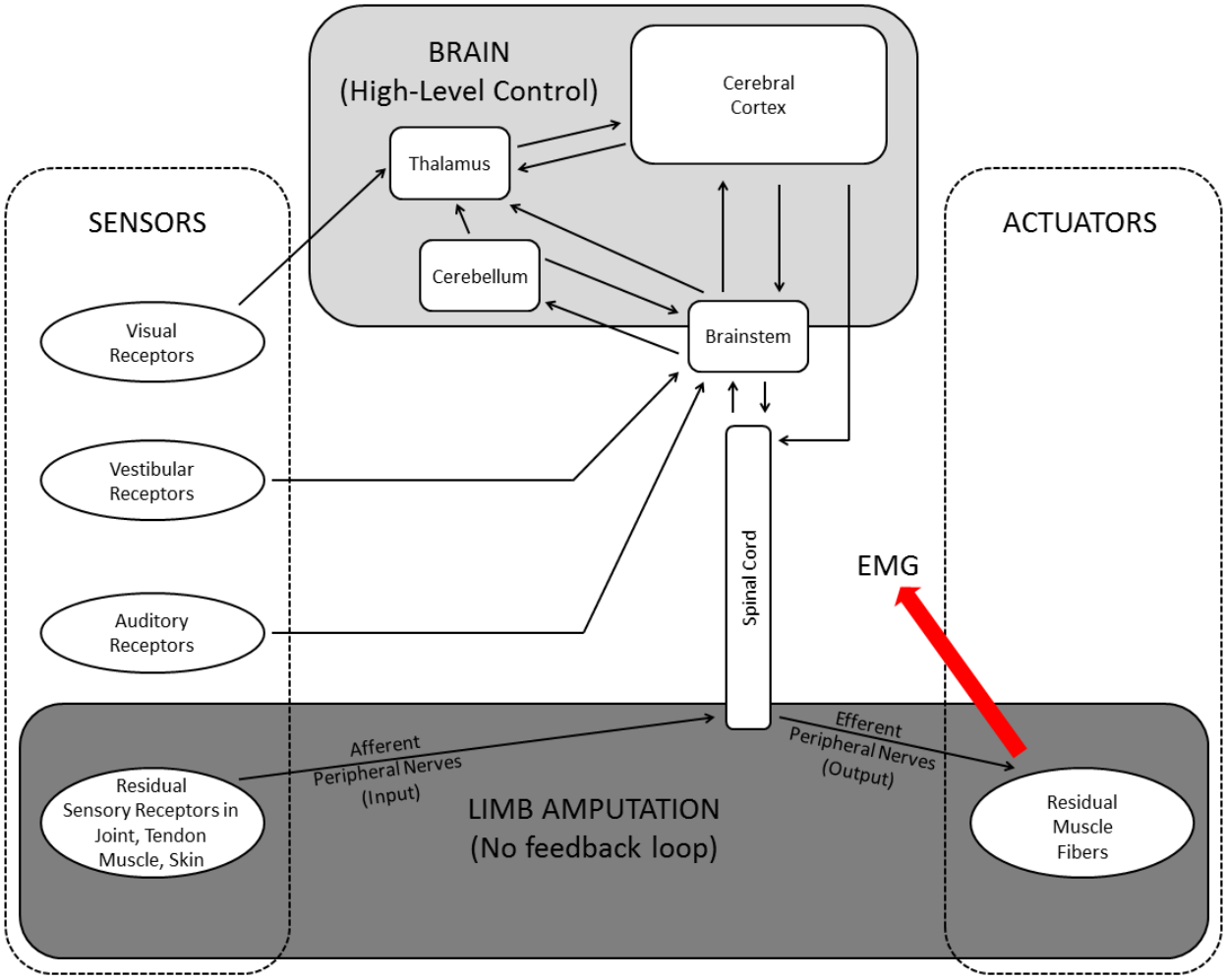

Figure 1.2. Effects of limb amputation in physiologic control of movement

5. Effects of Spinal Cord Injury on Control of Movement

In the case of a spinal cord injury, the actuators (muscles) and the sensory receptors are present, but the sensory information does not reach the high-level controllers, and the motor output signal does not reach the actuators (Figure 1.3). Some feedback loops, such as low-level spinal motor circuits, are intact below the injury, but they are not correctly regulated, as the signals regulating the circuits originate from above the injury level (Figure 1.3).

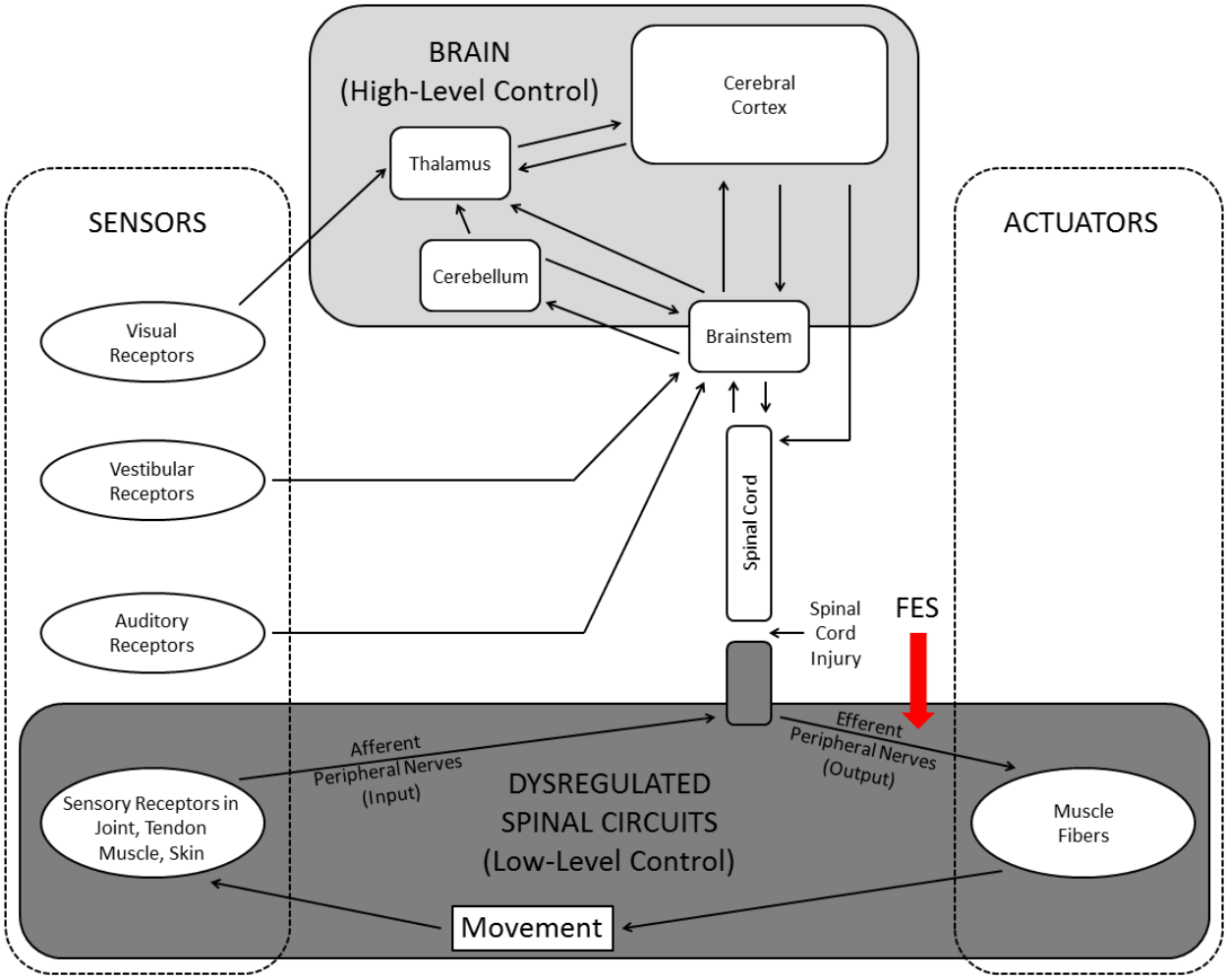

Figure 1.3. Effects of spinal cord injury in physiologic control of movement

6. Underlying Theme of the Presented Approaches

During the development of each control approach, the controller was designed so that an assistive device can compensate for impaired physiological functions in individuals with mobility impairments, while maximizing the use of retained physiological functions. Once the controller was found to be functional, it was simplified as much as possible (to the best of our knowledge) without compromising functionality. Overall, emphasis was given to practicality and usability, so that real users with mobility impairments would find the devices useful and benefit from using them.

CHAPTER II

VOLITIONAL CONTROL OF POWERED ASSISTIVE DEVICES

The control method presented in this chapter uses pattern recognition of EMG signals to convey the user's intent to powered prosthetic devices. Electric actuators in a powered prosthesis can provide the functionality of the user's muscles as actuators, while embedded sensors can provide sensory information for low-level control, in a similar manner to sensory receptors in the body. In order to achieve volitional control of a powered prosthetic device, the user's intent needs to be conveyed to the device in some form of physiological signals. The manuscript presented in this chapter describes a control method that uses EMG signals for high-level control of a powered transfemoral prosthesis exclusively for nonweight-bearing settings, while low-level control is achieved by closed-loop controllers within the device. Note that the approach is not intended for locomotive function, which is periodic and achievable with finite-state control structures. Rather, the approach described here is intended to provide purely volitional movement during activities such as sitting and non-weight-bearing standing. The presented control method uses a machine learning algorithm to minimize the need for manual calibration in the presence of noise and variations in EMG signals. This manuscript was published in the January, 2011 issue of the *IEEE Transactions on Biomedical Engineering*.

1. Manuscript 1: Volitional Control of a Prosthetic Knee Using Surface Electromyography

1.1 Abstract

This paper presents a method for providing volitional control of a powered knee prosthesis during non-weight-bearing activity such as sitting. The method utilizes an impedance framework, such that the joint can be programmed with a given stiffness and damping that reflects the nominal impedance properties of an intact joint. Volitional movement of the knee joint is commanded via the stiffness set-point angle of the joint impedance, which is commanded by the user as a function of the measured surface electromyogram (EMG) from the hamstring and quadriceps muscles of the residual limb. Rather than use the respective EMG measurements from these muscles to directly command the flexion or extension set-point of the knee, the presented approach utilizes a combination of quadratic discriminant analysis and principal component analysis to align the user's intent to flex or extend the knee joint with the pattern of measured EMG. The approach was implemented on three transfemoral amputees, and their ability to control knee movement was characterized by a set of knee joint trajectory tracking tasks. Each amputee subject also performed the same set of trajectory tracking tasks with his sound side (intact) knee joint. The average root mean square trajectory tracking errors of the prosthetic knee employing EMG-based volitional control and the intact knee of the three subjects were 6.2 and 5.2 degrees, respectively.

1.2 Introduction

Although prosthetic knee joints for transfemoral prostheses have traditionally been energetically passive devices, powered, semi-autonomous knee joints have recently started to emerge in the research community [8-10] and on the commercial market [11, 12]. While passive knee prostheses can only react to mechanical energy imparted by the amputee, powered knee prostheses have the ability to act independently of mechanical energy from the user. As such, the nature of the user communication with and the control of a powered prosthesis is substantially different from the control of a traditional, energetically passive prosthesis. Various methods have been presented in the engineering literature for the control of powered knee prostheses [8, 9, 13,

14]. These approaches utilize instrumentation on the prosthesis and/or the sound leg to form knee joint angle trajectories or impedances for the powered knee prosthesis to track while standing, walking, or transitioning between sitting and standing. All these methods rely on some form of physical input from the user for communicating with the powered knee prosthesis. That is, although the user need not provide the energy for movement (as is the case with traditional dissipative knee prostheses), the user must still provide physical input that can be measured by instrumentation on the prosthesis and/or sound leg (e.g., weight-bearing on the prosthesis, torque and/or acceleration from the affected-side hip joint, movement of the sound-side leg, etc.). In the absence of such physical input, the amputee is unable to convey intent to or provide control of the powered prosthesis.

1.2.1 Volitional Control of Powered Knee Prostheses

Note that activities such as standing, walking, or transitioning between sitting and standing all involve physical input and/or energy exchange between the residual limb and prosthesis. An important class of movement, however, which does not involve any significant physical input from the user, is the task of non-weight-bearing volitional control of knee movement while sitting or standing. That is, people regularly shift their body while sitting, often requiring significant movement of the knee joints. Such movement has both physiological and practical purposes. Regarding the former, weight shifting during sitting is known to play an important role in ensuring healthy circulation of blood in weight-bearing tissues [15]. Regarding the latter, sitting in confined areas, such as in automobiles, airplanes, theatres, and classrooms, often requires shifting of body position (particularly of the knee joints) in order to accommodate a particular ergonomic space and/or the movement of other individuals into or out of that space. Such movement is referred to herein as volitional control of the knee joint during non-weight-bearing activity. Note that such volitional control is also useful in non-weight-bearing standing, such as when flexing the knee to look at the bottom of a shoe, or when placing the foot on an elevated surface (such as a chair) to tie or untie, or don or doff a shoe. In the case of a traditional, energetically passive prosthesis, an amputee can achieve “volitional” control functionality by manipulating the prosthetic knee leg with his or her hands. Since a powered knee prosthesis has the capability to move itself, however, such artificial manipulation is fundamentally not required

for volitional movement of the knee joint. Despite this, since such activity does not involve significant physical input from the amputee, the previously cited control approaches do not provide an effective means of communication with the prosthesis. As such, this paper presents a method for the volitional control of the knee joint during non-weight-bearing activity which utilizes a pair of surface electromyogram (EMG) electrodes (on the ventral and dorsal aspects of the thigh, respectively), presumably integrated into the amputee's socket interface. Note that this approach is intended to be integrated with the impedance-based weight-bearing controllers for standing, walking, and transitioning between sitting and standing described in [8, 9], and as such is utilized only for the volitional control of the knee joint during non-weight-bearing activity. The approach for EMG-based volitional control of the knee is implemented on a powered knee prosthesis on three transfemoral amputee subjects. The ability of the amputee subjects to control knee movement is compared to their ability to move their sound knees during similar activity.

1.2.2 EMG-based Control of Lower Limb Prostheses and Orthoses

Other researchers have investigated the use of surface EMG for the control of lower limb prostheses and orthoses. In the case of passive knee prostheses, Horn [16] developed a prosthesis with an electrically activated knee flexion lock, and used surface EMG from the residual limb of a transfemoral amputee to trigger the engagement and disengagement of the lock. A similar approach was also reported by Saxena and Mukhopadhyay [17]. Aeyels et al. [18-20] developed a computer-controllable passive knee prosthesis based on an electrically modulated brake, and utilized surface EMG from three sites on the residual limb of a transfemoral amputee for gait mode recognition, which in turn was used to switch the prosthesis into the appropriate gait mode.

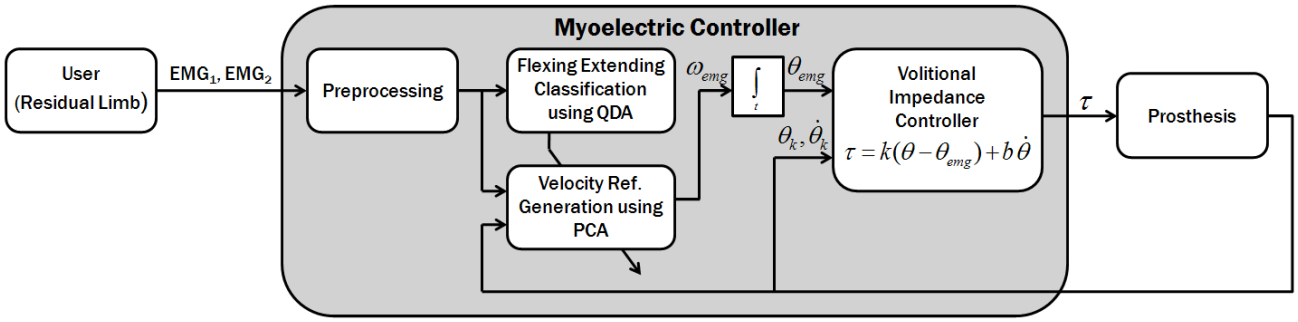

Figure 2.1. Block diagram of the myoelectric volitional impedance controller

More recently, Huang et al. [21, 22] utilized surface EMG from multiple electrodes on transfemoral amputees to classify movement intents while walking. With regard to using EMG for the real-time control of a powered knee prosthesis, the only prior work of which the investigators are aware is that of Donath [23], who attempted to use surface EMG from the quadriceps and hamstrings to control the motion of a hydraulically actuated powered knee prosthesis during walking. Donath concluded his study with the assertion that use of such an approach during gait would be challenging, due in part to difficulty in obtaining reliable EMG measurement "due to noise pick up and movement artifact." Other researchers have used surface EMG measured from the lower leg for the control of powered ankle joints in transtibial prostheses, or powered joints in ankle-foot orthoses (AFOs). With regard to the former, Au et al. [24] describe two approaches for predicting desired ankle movement from EMG measurement of the lower leg. As described in [25], Au et al. subsequently describe a control structure that relies only on physical input for control within a given activity mode, and uses EMG input to switch between the appropriate activity modes (and specifically between level walking and stair descent). With regard to powered AFOs, Ferris et al. [26-28] describe the use of EMG measured from the lower leg to control the assistive pressure in a pneumatically actuated AFO. Finally, Kawamoto and Sankai [29] describe a control system for an assistive exoskeleton with powered hip and knee joints, in which the assistive torque from the exoskeleton is proportional to the measured EMG from the associated flexion or extension muscles. The authors are not aware of any prior work utilizing EMG for the volitional control of knee joint motion in a powered knee prosthesis (aside from [23], which unlike the present work, attempted to use EMG for the real-time control of gait).

1.3 Volitional Control Structure

The volitional control framework is intended to provide volitional control of the knee with a joint output impedance similar to that of the native limb. As such, rather than use the measured EMG to prescribe joint torque, angle, or angular velocity, the presented framework utilizes measured EMG to prescribe the angular velocity of an equilibrium point of joint impedance that consists of the combination of a joint stiffness and damping. In this manner, the knee moves to a desired position with a joint output stiffness and damping prescribed by the controller, thus presumably moving in a more natural manner (relative to a high-output-impedance position controller), and resulting in a more natural interaction between the user, prosthesis, and environment.

The structure of the volitional controller is shown in Figure 2.1. Note that a real-time intent recognizer, such as the one described in [9], would be used to switch between this (volitional) controller and other weight-bearing control structures (such as those described in [8]). Note also that EMG is used to generate an angular velocity command (rate of change of the knee equilibrium point) rather than a position command, so that the user contracts the residual limb musculature only to move the joint and can relax when maintaining any given knee joint angle (as is commonly the case in upper extremity myoelectric control). Specifically, the joint torque command is given by:

$$\tau = k(\theta - \theta_{emg}) + b\dot{\theta} \tag{1}$$

where the equilibrium point θ_{emg} is given by

$$\theta_{emg} = \theta_o + \int_t \omega_{emg} dt \tag{2}$$

where k is the prescribed joint stiffness, b is the prescribed joint damping coefficient, θ is the knee joint angle, and θ_o is the initial angle when the control system switches to the volitional

(non-weight-bearing) controller and ω_{emg} is the angular velocity reference generated from the quadriceps and hamstring EMG, as described in the following section.

1.4 Reference Velocity Generation

The impedance controller utilizes the measured surface EMG from the quadriceps and hamstring muscles to generate a joint angular velocity reference, ω_{emg}, to drive the joint angular impedance equilibrium point, θ_{emg}, and thus to drive the motion of the knee. The simplest method for doing so would be to use

$$\omega_{emg} = \begin{cases} k_h e_h & \text{if} \quad e_h \geq e_q \\ -k_q e_q & \text{otherwise} \end{cases} \tag{3}$$

where e_h and e_q represent the measured (i.e., rectified and filtered) EMG from the hamstring and quadriceps muscles, respectively, and k_h and k_q are simple gains. Equation (3) also assumes that an appropriate deadband is applied to the measured EMG, to avoid "jitter" in the angular velocity reference command. Equation (3) is similar to the method used for the control of myoelectric upper extremity prostheses. Despite this, use of equation (3) provided only marginal performance in the presented volitional controller. Specifically, as described subsequently (and indicated in Figure 2.2), two of the three amputee subjects on which the approach was implemented demonstrated a significant degree of co-contraction when attempting to contract either the hamstrings or quadriceps in an isolated manner. With sufficient training, these subjects could possibly be trained to avoid co-contraction. Co-contraction, however, is a natural neuromuscular response (particularly in the lower limb musculature). As such, in an effort to render the volitional controller as natural as possible, the authors chose to train the controller to properly interpret co-contraction, rather than train the subjects to avoid it. Therefore, as indicated in the control structure of Figure 2.6 and described below, the controller first utilizes pattern classification to classify the user's intent with regard to flexion or extension of the knee, then utilizes a projection operator to extract the desired magnitude of the joint angular velocity reference from the measured EMG data.

1.4.1 Flexion-Extension Classification

As previously mentioned, rather than train the subjects to avoid co-contraction while commanding flexion or extension of the knee, the authors utilize a pattern classification approach to distinguish user intent to flex or extend the knee. In particular, the authors utilized a quadratic discriminant analysis (QDA) classifier to distinguish between the user's intent to flex or extend. Note that a linear discriminant analysis (LDA) classifier was also applied to the classification problem, although the QDA was chosen due to improved classification accuracy (based on the mean accuracy obtained with a five-fold cross-validation for each subject), and because the QDA is not significantly more complex (or computationally expensive) than the LDA classifier. Specifically, QDA uses the quadratic decision boundary of the form $c_1 + c_2e_h + c_3e_q + c_4e^2_h + c_5e_he_q + c_6e^2_q = 0$ to classify the sample consisting of the processed EMG data from the two channels, e_h and e_q, to the extension and flexion classes where the coeffiecients c_i, i=1,2,…,6 are generated during the training of the QDA classifier. Details of the LDA and QDA methods can be found in several pattern classification references, such as [30]. Note that a database of EMG (versus intent) data is required to parameterize the flexion/extension classifier, as described below.

1.4.2 EMG Measurement and Preprocessing

Although the eventual intent is to embed surface EMG electrodes in the prosthesis socket, for the implementation described herein, commercially available surface electrodes were used to acquire EMG signals from the residual quadriceps and hamstring muscles of the amputee subjects. The electrodes (B&L Engineering, model BL-AE-W, Santa Ana CA) were active bipolar units with dry contacts. Each electrode contained an integrated differential amplifier of gain 200 and a bandpass filter, with low and high roll-off frequencies of 10 and 3000 Hz, respectively. The distance between the poles within each electrode was 34 mm. Each electrode also included a (single) reference contact, located midway between the two poles. For each subject, electrodes were placed over the quadriceps and the hamstrings. Electrode locations were chosen to maximize the strength and reliability of signals while minimizing crosstalk from nearby muscles. Once the locations were determined, pictures were taken of the residual limb to ensure

consistency between sessions for electrode placement. The locations of electrodes varied slightly between subjects due to variations in post-surgical limb anatomy. The signals from the active electrodes were further low-pass filtered using a second-order analog filter with 5 Hz cutoff frequency. The filtered signals were then acquired by a computer running MATLAB Real Time Workshop at 1000 Hz sampling frequency using a 16-bit digital-to-analog converter card. The digital signals were processed using a first-order high-pass filter with 20 Hz cutoff frequency, a rectifier, and a first-order low-pass filter with 2 Hz cutoff frequency.

1.4.3 EMG Intent Database Generation

Generating a classifier training database consisted of recording 100 seconds of EMG data for knee flexion and 100 seconds for knee extension for each subject, with a one-minute rest in between, and thus the entire training session lasted less than five minutes. For each flexion/extension class, each subject was asked to visualize extending the knee on the amputated side at 0, 25, 50, 75 and 100 percent of full effort, several times for durations ranging from 1 to 5 seconds, over the total data collection period of 100 seconds at 100 Hz sampling frequency. The extension data was recorded first, followed by a rest period of approximately one minute, followed by the same procedure for flexion data. All EMG data was normalized into the interval [0, 1]. The data was additionally thresholded at 20% maximum effort, such that samples in the interval [0, 0.2] were effectively removed from the database, in order to mitigate baseline EMG noise and muscular tonicity. Based on this thresholded database, the QDA classifier was parameterized to classify each subject's preprocessed EMG as intent to either flex or extend the knee joint.

1.4.4 Reference Velocity Magnitude

The QDA provides a probabilistic optimal separation boundary of the EMG data to the flexion and extension classes. Within a given class (flexion or extension in this case), the "magnitude" of the data is the projection along the principal axis of that class. In the control approach described herein, this projection is generated via principal component analysis (PCA), which projects the two-dimensional EMG data along a principal (either flexion or extension) axis. Using the data

belonging to each class, two *2x2* PCA projection matrices W_E and W_F were computed. In the real-time implementation, one of these projection matrices was used to extract the "magnitude" information, based on the result of QDA classification as follows:

$$[x_p \; x_s]^T = \begin{cases} W_E \, [x_h \; x_q]^T & \text{if } \omega_{\mathrm{E}} \\ W_F \, [x_h \; x_q]^T & \text{if } \omega_{\mathrm{F}} \end{cases} \tag{4}$$

The magnitude of the angular velocity reference for the joint impedance set-point, ω_{emg}, is therefore the PCA-based projection of the two-dimensional EMG data along the principal axis of either the flexion or extension data. Details of PCA can be found in several references, such as [31]. Note that the projected EMG data is scaled between zero and the maximum reference velocity to generate the desired angular velocity reference. The maximum reference velocity is determined as the maximum reasonable angular velocity command for volitional control of the knee joint.

In contrast to (3), which obtains a reference angular velocity (for the volitional control impedance set-point) by projecting data along a hamstring/quadriceps set of measurement axes, the presented approach (which combines QDA classification with PCA projection of the two-dimensional EMG data) establishes a probabilistically optimal linear transformation from a hamstring/quadriceps set of axes to a flexion/extension set of axes (based on the training dataset). As such, the subject need not be trained to isolate the contraction of individual muscle groups but rather is free to co-contract the hamstring and quadriceps groups in a natural manner when intending knee flexion or extension.

1.5 Experimental Implementation

1.5.1 EMG-based Reference Velocity Generation

The volitional knee joint controller was implemented on three transfemoral amputee subjects. The subjects were all male, between the ages of 20 and 60, and between 3 months and 4 years

post amputation. Two subjects were unilateral transfemoral amputees, while one subject (subject 3) was a bilateral amputee, with a transfemoral amputation on one leg and a transtibial on the other. In all cases, all subjects were characterized by a prosthetic knee on one limb and an intact knee on the other. Note that all aspects of the study described herein were approved by the Vanderbilt Institutional Review Board, and all subjects signed informed consent forms prior to participation. Figure 2.2 shows the EMG intent database corresponding to each subject. Recall that these databases correspond to 100 seconds of flexion data at various degrees of (muscular) effort, and 100 seconds of extension data, also at various degrees of effort. Note that the x_q axis represents the measured, preprocessed, normalized, and thresholded EMG for the quadriceps group, while the x_h axis represents the EMG for the hamstring group. As seen in the figure, two of the three subjects (subjects 1 and 3) demonstrated a significant amount of muscular co-contraction when intending volitional movement of the prosthetic knee. Interestingly, subject 1 primarily demonstrated significant co-contraction during intent to extend the knee, while subject 3 primarily demonstrated significant co-contraction during intent to flex the knee. For all subjects, the LDA and QDA boundaries between classes along with the pseudo-classification boundary described by (3) are shown in the figures. Recall that, based on a five-fold cross-validation of classification accuracy, QDA classification in general provided higher classification accuracies, and therefore was used in the control experiments to classify intent to flex or extend the knee. Specifically, the mean accuracies of the classifiers over 5 CV-fold for each of the three subjects were 0.99, 0.80 and 0.86 for the LDA and 1.0, 0.86 and 0.90 for the QDA. Note that, particularly in the cases of subjects 1 and 3, the simple thresholding approach (described by (3)) entails a considerable amount of erroneous "classification" of intent, even in the case of large amplitude EMG ($x_i > 0.3$). In contrast, the QDA classification boundaries entail little to no classification error, particularly in large amplitude EMG.

Once intent to flex or extend the knee is known, the magnitude of the angular velocity for the impedance set-point is obtained by projecting the corresponding data point onto its principal axis via PCA. A representative example of the corresponding PCA projections for subject 1 is shown in Figure 2.3. In the figure, the x_p axis corresponds to the PCA projection of the flexion and extension data along the principal component of that data. As such, the angular velocity for the impedance set-point of the volitional knee joint controller is given by:

$$\omega_{emg} = \begin{cases} 0 & \text{if } \omega_{\mathrm{F}} \text{ and } (x_P < \gamma) \\ \alpha\left(\dfrac{x_p - \gamma}{1-\gamma}\right) & \text{if } \omega_F \text{ and } (x_P \geq \gamma) \\ 0 & \text{if } \omega_{\mathrm{E}} \text{ and } (x_P < \gamma) \\ -\alpha\left(\dfrac{x_p - \gamma}{1-\gamma}\right) & \text{if } \omega_E \text{ and } (x_P \geq \gamma) \end{cases} \tag{5}$$

where α is the maximum desired set-point velocity (corresponding to maximum muscular effort), γ is the value at which the normalized EMG is thresholded (in this case γ = 0.2), x_p is the PCA projection along the principal axis (as shown in Figure 2.3).

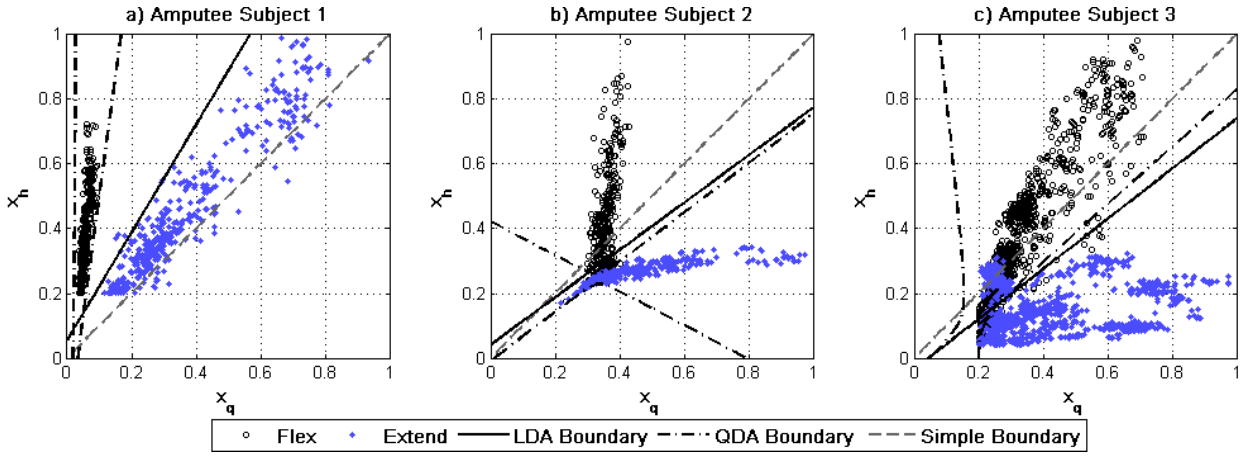

Figure 2.2. Classification of extension and flexion reference signals using QDA and LDA for amputee subjects 1, 2 and 3 (Figures a, b and c). Simple boundary depicts the pseudo-classification boundary if the simple control rule in (3) is used. x_q and x_h denote the normalized EMG signals for the quadriceps and hamstring muscles, respectively.

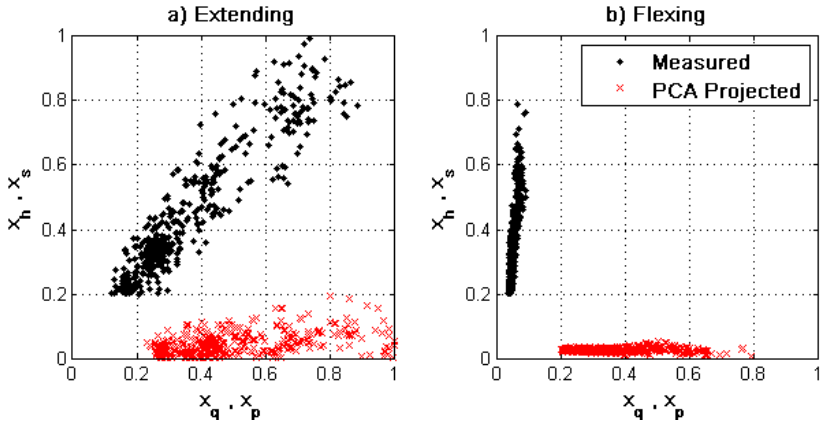

Figure 2.3. PCA projections of extension (a) and flexion (b) reference signals of amputee subject 1. For the actual samples (measured), x_q and x_h denote the normalized EMG signals for the quadriceps and hamstring muscles, respectively. For the PCA projections, x_p and x_s denote the first principal and second principal components, respectively.

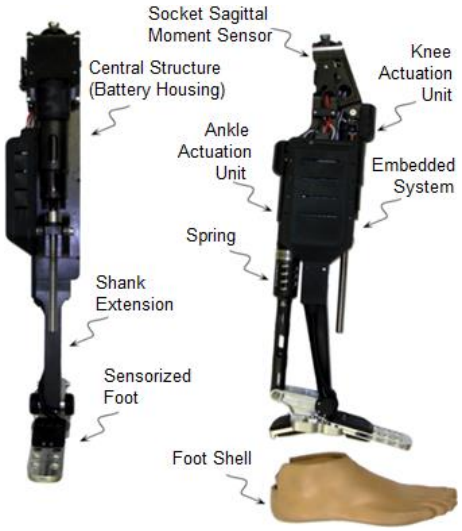

Figure 2.4. The powered transfemoral prosthesis.

1.5.2 Volitional Trajectory Tracking of a Powered Knee Prosthesis

The volitional knee controller was implemented on each of the three amputee subjects with the powered transfemoral prosthesis shown in Figure 2.4 and described in detail in [8]. Note that the prosthesis used in these experiments also contains a powered ankle, although the ankle was not explicitly commanded in these experiments and remained in a "neutral" configuration. In order to characterize the effectiveness of the volitional controller for purposes of moving the knee joint, an experiment was developed which required each subject to track various types of knee joint angle movements. During these experiments, each amputee was presented with a computer monitor that showed in real-time a desired knee angle as a trajectory, along with the knee angle of the powered prosthesis, as measured by the joint angle sensor on the prosthesis. Since the authors did not have prosthesis sockets with embedded EMG electrodes for each subject, and since the volitional controller is intended for non-weight-bearing activity such as sitting, the subjects did not wear the powered prosthesis during the knee control experiments, but rather the subjects were seated in a chair, with the powered knee prosthesis mounted to a bench immediately next to the subject, in an orientation that was consistent with their seated position. The subjects were free to shift their weight and reposition the residual limbs during the sessions, and no significant changes in the EMG signals were observed. Aside from the QDA and PCA parameters extracted from the EMG intent database, all subjects utilized the same set of

volitional control parameters for the powered prosthesis. Specifically, the stiffness of the impedance controller was selected as k = 1.0 Nm/deg, the damping as b = 0.01 Nm/deg/s, the maximum set-point velocity α = 50 deg/s. These parameters were selected experimentally to provide an acceptable bandwidth and natural appearance of motion.

In order to characterize volitional control of various types of motion, four different desired trajectories were constructed (labeled as trajectories *A* through *D*). The trajectory *A* joint angle tracking task consisted of set-point trajectories requiring the subject to quickly change the knee angle in 8 to 45 degree increments and to hold it for 5 to 10 seconds. Trajectory *B* consisted of sloped trajectories, which were intended to measure the subject's ability to move the prosthesis at different constant velocities. Trajectories *C* and *D* consisted of sinusoidal waves at 0.2 and 0.33 Hz, respectively (i.e., five-second and three-second periods, respectively), which were intended to measure the subject's ability to move the leg up and down smoothly at continuously varying velocities. Trajectories *A* and *B* lasted for a total duration of 160 seconds each, while trajectories *C* and *D* lasted for a total duration of 80 seconds each.

For each amputee subject, three sessions of experiments were conducted, each on a different day, with each successive session approximately one week apart. During the experimental sessions, the amputee spent approximately one hour practicing the tracking of the four trajectories (*A* through *D*), during which the various trajectories were presented to the amputee in an arbitrary order. After completion of the third session (i.e., after approximately one hour of practice in the third session once the experimenters concluded that the subject's performance had plateaued), the subject's performance was evaluated in a single set of performance tests, consisting of one trial each of trajectories *A* through *D*. Trajectory tracking performance data for all three subjects for these four trajectories is shown in Figure 2.5. The mean root mean square (RMS) trajectory tracking error for each amputee subject for each of the four trajectories is summarized in Table 1. The last column shows the average RMS trajectory tracking error across the three subjects, along with the standard deviation corresponding to the respective means. Finally, Table 1 also shows the average RMS tracking error across all subjects and all trajectories (i.e., mean of the last column), along with the corresponding standard deviation, which are 6.2 deg and 0.71 deg,

respectively. The latter indicates similar levels of tracking performance between the three subjects (which is also evidenced in Figure 2.5).

1.5.3 Comparison to Intact Knee Trajectory Tracking

In order to provide context for the trajectory tracking data summarized in Table 1, corresponding experiments were conducted to assess the ability of each amputee to track the same set of knee joint angle trajectories with his sound knee. These experiments were conducted in a single session, since familiarization with the prosthesis and volitional impedance controller was not necessary (i.e., each subject was already quite familiar with the movement control of his sound knee). As such, each subject spent approximately 15 minutes practicing each set of trajectories, until each was comfortable with his ability to track the trajectories. Once sufficiently comfortable, each subject's performance was evaluated in a single set of performance tests, consisting of one trial each of trajectories *A* through *D*. Movement of the sound knee was measured using a knee brace instrumented with a goniometer. The knee brace did not impose any significant constraints on knee movement. Intact knee trajectory tracking data for all three subjects (whose prosthetic side data is shown in Figure 2.5) for the four trajectories is shown in Figure 2.6, and a summary of the mean RMS errors for the intact knee (corresponding to Table 1) is given in Table 2. As shown in the last column of Table 2, the average RMS tracking error across all subjects and all trajectories for sound knee tracking was 5.2 deg, with a corresponding standard deviation of 1.0 deg. Recall that the average RMS tracking error across all subjects and all trajectories for the EMG-based prosthesis knee tracking was 6.2 deg (with a standard deviation of 0.71 deg). Thus, the data indicates that all three subjects performed similarly (i.e., relatively small standard deviation relative to the respective means), and that on average, the difference in tracking error between the prosthetic and intact knee joints was one degree. With regard to the various trajectory types, the average RMS errors for trajectory *A* (steps) were 7.7 deg and 6.8 deg, respectively, for the prosthetic and intact joints, and thus the difference in average error was 0.9 deg. The average RMS errors for trajectory *B* (ramps) were 3.4 deg and 2.1 deg, respectively, for the prosthetic and intact joints, and thus the difference in average error was 1.3 deg. For trajectory *C* (the slower sinusoid), the average RMS errors were 5.6 deg and 5.7 deg, respectively, for the prosthetic and intact joints. Despite this, the standard deviation in the

average RMS error was significantly different between the two, indicating that the sound side tracking of the slow sinusoid was more consistent between the three subjects than the prosthetic side. Finally, for trajectory *D* (the faster sinusoid), the average RMS errors were 7.9 deg and 6.2 deg, respectively, for the prosthetic and intact joints, and thus the prosthesis controller demonstrated 1.7 deg more error on average than the intact joint.

Table 1: RMS Error for EMG Control of Powered Knee

	Subject 1 EMG	Subject 2 EMG	Subject 3 EMG	EMG Control Avg. (SD)
Trajectory A	6.8	8.2	8.0	7.7 (0.76)
Trajectory B	2.5	3.9	3.7	3.4 (0.76)
Trajectory C	4.4	7.2	5.3	5.6 (1.4)
Trajectory D	8.4	8.3	7.1	7.9 (0.72)
Subject Avg.	5.5	6.9	6.0	6.2 (0.71)

Table 2: RMS Error for Volitional Control of Intact Knee

	Subject 1 Sound	Subject 2 Sound	Subject 3 Sound	Sound Side Avg. (SD)
Trajectory A	6.1	6.8	7.6	6.8 (0.75)
Trajectory B	1.4	1.8	3.1	2.1 (0.89)
Trajectory C	4.6	6.1	6.4	5.7 (0.96)
Trajectory D	4.5	6.4	7.7	6.2 (1.6)
Subject Avg.	4.2	5.3	6.2	5.2 (1.0)

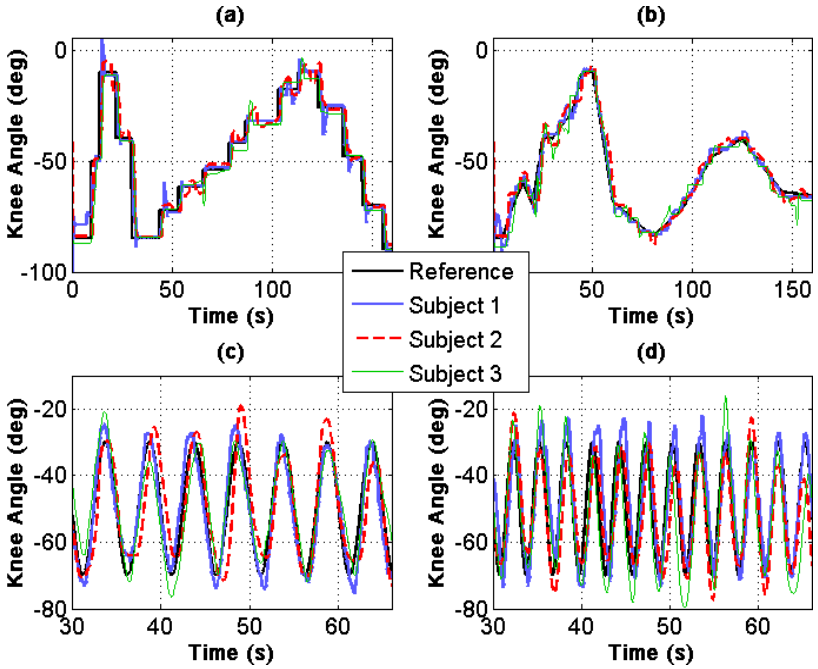

Figure 2.5. EMG-controlled powered prosthesis knee position tracking for all three subjects for trajectories *A-D* (Note that *C* and *D* show only a segment of the longer sinusoidal trajectory.).

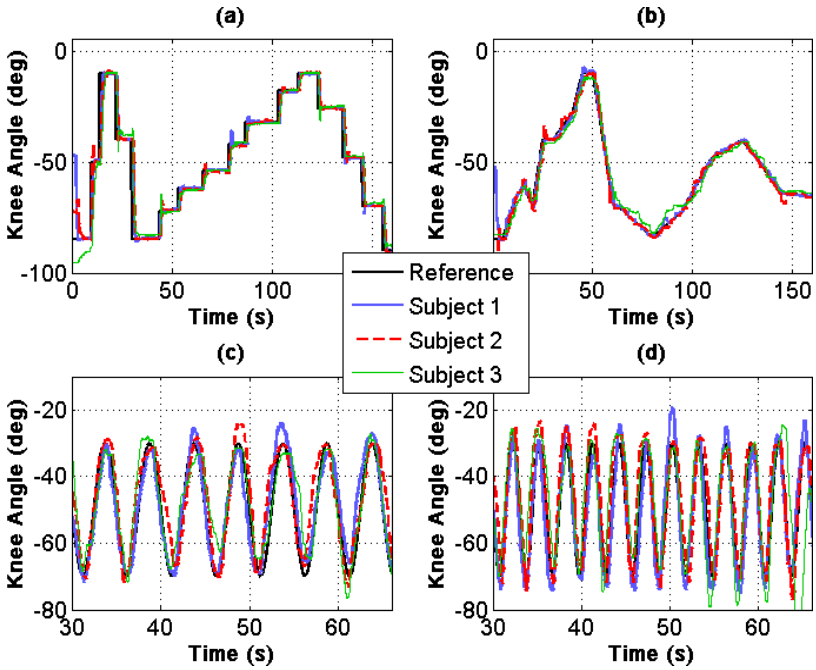

Figure 2.6. Sound-side knee position tracking for all three subjects for trajectories *A*-*D* (Note that *C* and *D* show only a segment of the longer sinusoidal trajectory.).

1.6 Conclusion

This paper describes a volitional impedance control framework that allows a transfemoral amputee to control the motion of a powered knee prosthesis during non-weight-bearing activity. The control is based on an impedance framework wherein the joint exhibits programmable joint stiffness and damping characteristics, and knee movement is provided by commanding the joint stiffness equilibrium angle. The time rate of change of this angle (which is the desired angular velocity) is provided by measurement of the surface EMG from the hamstring and quadriceps muscles. Rather than directly associate the hamstring EMG with knee flexion and the quadriceps with knee extension, which would require the user to artificially isolate contraction of these muscle groups, the approach incorporates a combination of pattern classification and principal component projection to align the measured EMG with the user's desire to flex or extend the knee joint. The resulting control approach was implemented on three transfemoral amputee subjects, and the resulting EMG volitional control was shown to provide effective control of knee joint motion during non-weight-bearing activity. The proposed approach, if implemented with EMG electrodes embedded into the socket, can provide amputees using powered knee

prostheses with the ability to perform effective volitional control of knee joint motion during non-weight-bearing activity.

1.7 Acknowledgment

The authors would like to thank M.A. Bulow, C.P. for his assistance in recruiting subjects.

CHAPTER III

ENHANCING A WALKING CONTROLLER FOR LOWER LIMB EXOSKELETONS TO ENABLE INCREASED WALKING SPEEDS

In the previous chapter, the user's intent was conveyed to the device using physiological signals (EMG). The control method presented in this chapter does not directly interface with the user's physiological signals but rather uses embedded sensors in the device to convey the user's intent to the device, which, in this case, is a lower limb exoskeleton for gait restoration in paraplegic individuals. A powered lower limb exoskeleton containing actuators, sensors, and microcontrollers can perform consistent motions in a similar manner to the low-level control of spinal circuits. Although such an exoskeleton attached to an individual with paraplegia can override the dysregulated spinal circuits in the body, the low-level controllers in the device are still disconnected from the person's high-level controllers (i.e. the brain). The manuscript presented in this chapter describes a high-level step trigger method for level-ground walking using information from inertial measurement units (IMUs) within the exoskeleton. The controller takes the user's dynamics into account based on a simple inverted pendulum model in order to improve gait speed. This manuscript is ready for submission to a journal to be determined.

1. Manuscript 2: Toward the Use of Robotic Exoskeleton to Facilitate Community Ambulation for Individuals with Paraplegia

1.1 Abstract

Recent advances in robotics technology have enabled the emergence of powered exoskeleton devices that have the potential to enable community or limited community ambulation for people with paraplegia. Preliminary studies published to date, however, indicate that these systems provide average walking speeds well below those generally prescribed for community or limited community ambulation. In order to increase walking speed, this paper proposes a dynamic control component that leverages knowledge of user dynamics to enable a more dynamic form of walking. The dynamic control approach is implemented on an exoskeleton and compared to the non-dynamic (quasi-static) control approach on a single subject with thoracic-level motor complete spinal cord injury (SCI), and is shown to improve average walking speed by a factor of more than two. In order to demonstrate efficacy of the control approach across multiple subjects, the exoskeleton and dynamic controller were assessed on four additional individuals with thoracic-level motor complete SCI, and were shown to provide similar gait speeds across all subjects. The average gait speed across all subjects was 0.37 m/s, which approaches (although does not fully achieve) the range of walking speed generally prescribed for limited community and community ambulation. The paper also reports results of other mobility assessments on the five subjects performed with the dynamic controller, such as the timed up-and-go and six-minute walk tests.

1.2 Introduction

The inability to stand and walk is one of the most significant impairments resulting from paraplegia [32]. In addition to diminished mobility, the inability to stand and walk can entail significant health implications, including loss of bone mineral content, pressure-induced skin problems, impaired lymphatic and vascular circulation, impaired digestive function, reduced respiratory and cardiovascular capacities, muscle spasticity, and increased incidents of urinary tract infection [7, 33-38].

In an effort to restore legged locomotion to individuals with spinal cord injuries, some researchers have developed robotic lower limb exoskeletons to facilitate walking, utilizing external power (e.g., a battery pack) in combination with joint actuators (e.g. electric motors) to provide motive power. Some of the efforts in this regard include [39-48]. While these devices have been shown to be capable of providing legged mobility, few studies have been reported on mobility assessment of these devices on paralyzed individuals. To the best of the authors' knowledge, two papers have published employing standard mobility assessment instruments to assess the legged mobility of paralyzed individuals using powered exoskeleton devices. One of these papers, by Esquenazi et al., reports average walking speed of 0.25 m/s (SD, 0.15 m/s), as measured by the ten-meter walk test (10mWT), in 11 subjects with thoracic-level paraplegia [49]. The other paper, by Farris et al. (i.e., essentially by the authors of this paper), compares ambulation with KAFOs to ambulation with a lower limb exoskeleton in a single subject with T10 complete paraplegia, and reports average walking speed with the exoskeleton of 0.17 m/s, as measured by a series of 10mWTs [50]. According to one study, the minimum gait speed necessary for community ambulation is 0.49 m/s, mainly due to time limits at crosswalks [51]. Another study prescribes a gait speed of 0.4 m/s for *limited* community ambulation [52]. In both cases, it is reasonable to assert that the reported average gait speeds of 0.17 to 0.25 m/s for exoskeleton walking are substantially below the gait speeds of 0.4 to 0.49 m/s generally prescribed for limited community and community ambulation (respectively).

In order to improve speed (with the intent of enabling limited community or community ambulation), the authors describe here a modification to the control method presented in Farris et al. that introduces a dynamic model to facilitate a dynamic initiation of each subsequent step, and thus to foster a more dynamic form of locomotion. After developing the dynamic approach, the controller is implemented on an exoskeleton and the resulting gait speed compared on a single subject to the (previously reported) non-dynamic control approach, and is shown to improve walking speed by more than a factor of two. The modified controller is then implemented on five thoracic-level subjects and shown to provide a highly consistent gait speed across these five subjects.

1.3 Materials and Methods

1.3.1 Controller

As described in detail in [47], walking in the exoskeleton is controlled by a finite state machine (FSM), consisting of four essential states, as illustrated in Figures 3.1 and 3.2, which are right step (state 1), double-support with right foot forward (state 2), left step (state 3), and double-support with left foot forward (state 4). During normal walking, the state machine moves sequentially through these states in a repeating fashion. When a right step is triggered (i.e., when state 1 is entered), the exoskeleton executes predetermined joint angle profiles (given in [47]), which executes swing phase in the right leg and stance phase in the left. Once the right step has completed, the FSM enters state 2, which is double-support with the right foot forward. When a left step is triggered, the exoskeleton executes joint angle profiles corresponding to left leg swing phase and right leg stance phase, and once completed, the FSM enters state 4, which is double-support with left foot forward. Therefore, when walking the controller moves fluidly through states 1 and 3 (right and left step), then waits in states 2 and 4 (double-support) for the user to trigger the subsequent step. The primary purpose of waiting in double-support for the user to trigger the subsequent step is to ensure that the user's postural configuration is such that taking a step will result in movement forward, rather than falling backward. In the control approach reported previously (17), the condition for triggering a step was based on the user's center of pressure (CoP), which is the vertical projection of the user's center of mass (CoM) onto the floor in the sagittal plane, falling in front of the forward foot. In the simplified model of walking depicted in Figure 3.3, this condition corresponds to triggering a subsequent step when $\theta \leq 0$, where θ is the angle of the user's stance leg in the vertical plane. This ensures that, when the exoskeleton performs joint motions for taking a step, the user steps forward, rather than fall backward. While this trigger method ensures that the user steps forward, it also requires that the user shift his or her CoP (using his or her arms and stability aid) far enough forward to meet this condition every step, which requires a deliberate effort and additional time between steps. The additional time between steps required to meet this condition has a substantial influence on walking speed.

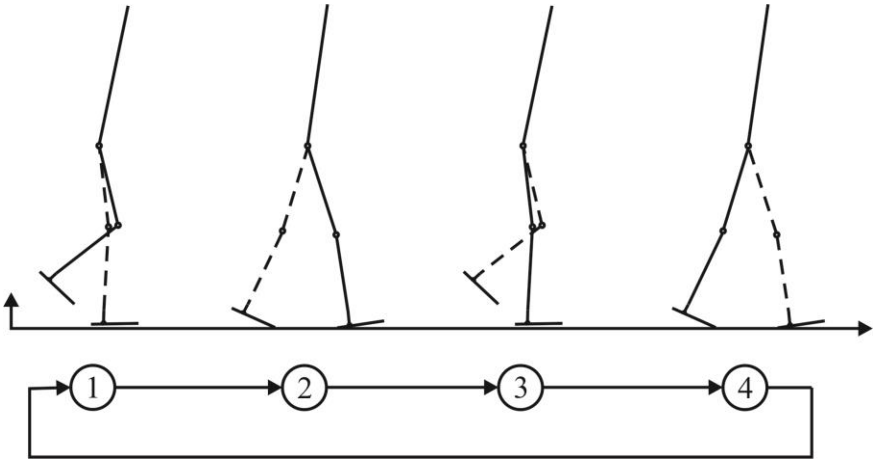

Figure 3.1. The finite state machine with four states involved in walking: right step (state 1), double-support with right foot forward (state 2), left step (state 3), and double-support with left foot forward (state 4).

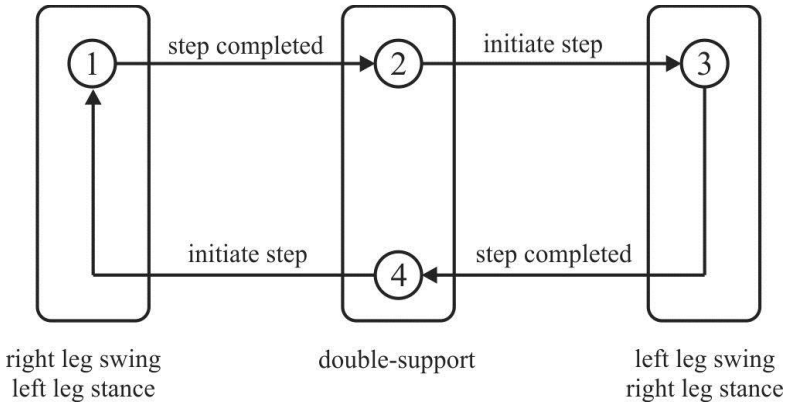

Figure 3.2. FSM for exoskeleton walking

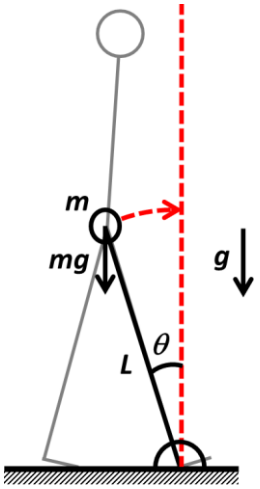

Figure 3.3. Updated step trigger method. The system is modeled as an inverted pendulum rotating about the stance foot, and a step is triggered if there is enough kinetic energy to overcome the potential energy needed to step forward.

Recognizing that healthy walking is characterized by dynamic movement, the authors modified the previously implemented step trigger to account for a simple model of the user dynamics. Rather than require the CoP to fall forward of the forward foot, the dynamic step trigger uses a simple model of the user to estimate the user's forward kinetic energy, and initiates a step when the user's CoP, in combination with his or her estimated kinetic energy, will result in forward movement. Specifically, the approach is based on the dynamics of a simple inverted pendulum (Figure 3.3), and a step is triggered if

$$KE \geq PE \tag{1}$$

where *KE* is the kinetic energy of the system and *PE* is the potential energy difference between the current position and the highest point of the inverted pendulum. In this model,

$$KE = \frac{1}{2} mL^2 \dot{\theta}^2 \tag{2}$$

where m is the mass of the system, L is the distance from the stance foot to the center of mass, and $\dot{\theta}$ is the angular velocity of the user's stance leg rotating about the stance foot. Similarly, in this model,

$$PE = mgL(1 - \cos\theta) \tag{3}$$

where g is the gravitational constant, and θ is the angle of the user's stance leg in the vertical plane. Substituting equations 2 and 3 into equation 1 gives the condition for triggering a subsequent step:

$$\dot{\theta}^2 \geq \frac{2g}{L}(1 - \cos\theta) \tag{4}$$

Note that, for quasi-static movement ($\dot{\theta} \cong 0$), this condition reduces to the same used previously (i.e., step is triggered when $\theta \leq 0$). As the user moves with increasing forward (i.e., angular)

velocity, however, the step trigger should occur increasingly earlier, while still maintaining the safety assurance of moving forward.

1.3.2 Exoskeleton

The dynamic walking control approach was implemented on the Vanderbilt lower limb exoskeleton, which is shown in Figure 3.4. The exoskeleton incorporates four control actuators (brushless DC motors acting through speed reduction transmissions) that provide sagittal-plane torques at the right and left hip and knee joints (relative to the exoskeleton frame). The control actuators are capable of providing continuous torques at each joint of approximately 20 N·m, and peak torques of approximately 80 N·m for durations on the order of a few seconds (thermally limited). The exoskeleton is used with ankle foot orthoses (AFOs), which provide stability at the ankle joints and transfer the weight of the exoskeleton to the ground. Instrumentation (for measurement of configuration angles, equation 4, and of state machine switching conditions, Figure 3.3) include absolute and incremental encoders at each joint, and one six-axis inertial measurement unit (IMU) in each thigh link (i.e., two total). The exoskeleton is powered by a 30 v, 120 W·hr lithium polymer battery with a mass of approximately 600 g. The total mass of the system, including the battery, is approximately 12 kg (26.5 lb). A more detailed description of the exoskeleton is provided in [53].

Figure 3.4. Vanderbilt lower limb exoskeleton

1.3.3 Preliminary Validation of Dynamic Walking Control Approach

In order to provide a preliminary validation of the dynamic walking step trigger, the dynamic walking step trigger was implemented on the lower limb exoskeleton and compared to the non-dynamic (quasi-static) step trigger, on a single subject with thoracic-level motor complete spinal cord injury (SCI). The subject, listed as Subject 1 in Table 3, was a 43-year-old male, 11 years post a T10 AIS A spinal cord injury. The subject is shown walking in the exoskeleton in Figure 3.5 (note that the subject gave permission for publication of the photograph). In the validation testing, walking speed was measured using the 10mWT, in which the subject was instructed to "walk as fast as you safely can" over a 14 m distance, with the middle 10 m segment being timed to determine walking speed. The test was repeated three times for each step trigger. The subject was allowed to rest fully between trials, and specifically was required to achieve a resting hearting rate prior to beginning the next 10mWT. As reported in Table 4, the mean walking speed for the three 10mWT using the quasi-static step trigger was 0.17 m/s (with a standard deviation, SD, of 0.01), while the mean walking speed with the dynamic trigger (equation 4) was 0.37 m/s (SD, 0.02). As such, the walking speed was more than doubled with the dynamic walking trigger, while the variation in walking speed across trials remained small (i.e., walking speeds were quite consistent using both step trigger methods). Note that in these trials, rather than using a measured value for the distance from the stance foot to the center of mass, the length L in equation 4 was approximated at 1 m.

Figure 3.5. Subject 1 walking using the exoskeleton

Table 3: Summary of Subject Profiles

	Subject 1	Subject 2	Subject 3	Subject 4	Subject 5
ASIA Impairment Scale	AIS A (Complete)	AIS A (Complete)	AIS A (Complete)	AIS A (Complete)	AIS B (Sensory Incomplete)
Injury Level	T10	T10	T8	T11	T6
Years since Injury	11	3	4	4	2
Gender	Male	Male	Male	Male	Male
Age	43	41	41	30	19
Height (m)	1.85	1.83	1.75	1.83	1.75
Weight (kg)	75	100	82	64	54

Table 4: Three-run Average (SD) Mobility Data for Subject 1: Previous vs. Updated Step Trigger Method

	Previous Step Trigger (Static)	Updated Step Trigger (Dynamic)
10mWT		
Time (s)	58 (3.1)	27 (1.2)
Speed (m/s)	0.17 (0.01)	0.37 (0.02)
6MWT		
Distance (m)	64 (4.5)	97 (0.58)

1.3.4 Assessment of Dynamic Walking in Multiple Subjects

In order to demonstrate efficacy of the dynamic walking control approach across multiple subjects, the exoskeleton and dynamic controller were assessed on four additional individuals with thoracic-level motor complete SCI (i.e., a total of five subjects with thoracic-level motor-complete injuries). Table 3 provides information regarding the injuries and other essential characteristics of the five subjects. As indicated in the table, all subjects had injuries ranging from T6 to T11, four had sensory and motor complete injuries (AIS A), and one had a sensory incomplete injury with no motor function below the level of injury (AIS B).

In addition to using the 10mWT, the exoskeleton and dynamic walking controller were additionally assessed by using as assessment instruments the six-minute walk test (6MWT), and timed up-and-go (TUG) test. While the 10mWT provides a measure of the gait speed over a short distance, the 6MWT measures the gait speed over a longer distance and duration, and also involves turns, whereas the 10mWT only involves walking in a straight line. The TUG test characterizes a person's ability to perform transitions between basic movements, such as sit-to-stand, stand-to-walk, walk-to-stand, turn in place, and stand-to-sit. The 10mWT, 6MWT, and

TUG test have all been shown to have high test-retest correlation coefficients (all around 0.98) and high levels of validity in assessing the functional mobility in individuals with neurological impairment [54-57]. Each subject repeated each tests three times, and each after heart rate returned to resting. All assessments were conducted at Shepherd Center, Atlanta, GA, between April 2013 and December 2013, with approval from the Shepherd Center and Vanderbilt University IRBs. Note also that, rather than use a measured value for the distance from the stance foot to the center of mass for each subject, the length L in equation 4 was approximated as 1 m for all trials and all subjects.

1.4 Results and discussion

Table 5 summarizes results for each assessment instrument, and for each subject. The average walking speed across all subjects, as measured by the 10 mWT, was 0.37 m/s (SD, 0.04). Average speeds for each subject ranged from 0.32 m/s to 0.42 m/s. The distance covered in 6 minutes averaged 97.8 m (SD, 10) and ranged from 89.8 m to 111.9 m. Note that since the 6MWT used 30.5 m (100 ft) spans between turning points, completing the 6MWT required each subject on average to complete 3 turns. Given the control system as described in (17), each turn requires that the subject transition from a walk state to a standing state; turn in place; then transition from a standing state to a walking state. The time required to complete each turn reduces the average walking speed substantially. The TUG tests were on average completed in 72.4 s (SD, 14), with times ranging from 56.3 s to 96.8 s. Note that the TUG test consists of transitions between standing, walking, turning, walking, turning, and sitting down, and thus the amount of walking is small relative to other activities. Nonetheless, the ability to independently complete a TUG test is an important indicator of potential for home and community use.

Table 5. Three-run Average (SD) Mobility Data for Five Subjects

	Subject 1	Subject 2	Subject 3	Subject 4	Subject 5	Average
10mWT						
Time (s)	27.4 (1.2)	23.9 (0.9)	29.3 (1.1)	26.2 (0.5)	30.5 (0.7)	27.6 (2.7)
Speed (m/s)	0.37 (0.02)	0.42 (0.02)	0.33 (0.01)	0.38 (0.01)	0.32 (0.01)	0.37 (0.04)
6MWT						
Distance (m)	96.9 (0.6)	111.9 (12.5)	90.0 (1.9)	89.8 (2.9)	100.5 (5.9)	97.8 (10)
TUG Test						
Time (s)	96.8 (4.2)	69.0 (3.7)	69.1 (1.5)	70.6 (6.9)	56.3 (1.3)	72.4 (14)

1.5 Conclusion

Ideally, an exoskeleton system should provide walking speeds appropriate for community or limited community ambulation. This study proposed a walking controller that enables a dynamic form of exoskeleton walking, which was shown to increase walking speed by a factor of two relative to a non-dynamic controller. The control approach was additionally shown to provide highly consistent walking speeds across five subjects with thoracic-level motor-complete injuries of varying levels, with an average walking speed (0.37 m/s) that approaches the range of speeds (0.40 to 0.49 m/s) prescribed for limited community and community ambulation. Despite this, the walking speeds achieved in this study remain on average somewhat below those prescribed for community or limited community ambulation.

CHAPTER IV

COOPERATIVE CONTROLLER COMBINING FES WITH POWERED EXOSKELETONS

While the previous work showed that a person with paraplegia could walk in a safe and consistent manner using a powered exoskeleton, the electric motors in the exoskeleton were the only sources of motive power, and the user's joints were simply moved in a passive manner. If the user's own muscles could also be used to create movement, the user might receive greater degrees of physiological benefits, in addition to reducing battery power consumption. The manuscript presented in this chapter uses functional electrical stimulation (FES) of paralyzed muscles as sources of actuation along with the electric motors of a powered exoskeleton, and a cycle-to-cycle adaptation ensures that the two types of actuators work together to achieve safe and efficient gait in individuals with paraplegia. This manuscript has been accepted for publication in the *IEEE Transactions on Neural Systems and Rehabilitation Engineering*. An addendum to this chapter describes the circuit design of the muscle stimulator used in this study.

1. Manuscript 3: An Approach for the Cooperative Control of FES with a Powered Exoskeleton during Level Walking for Persons with Paraplegia

1.1 Abstract

This paper describes a hybrid system that combines a powered lower limb exoskeleton with functional electrical stimulation (FES) for gait restoration in persons with paraplegia. The general control structure consists of two control loops: a motor control loop, which utilizes joint angle feedback control to control the output of the joint motor to track the desired joint trajectories, and a muscle control loop, which utilizes joint torque profiles from previous steps to shape the muscle stimulation profile for the subsequent step in order to minimize the motor torque contribution required for joint angle trajectory tracking. The implementation described here incorporates stimulation of the hamstrings and quadriceps muscles, such that the hip joints are actuated by the combination of hip motors and the hamstrings, and the knee joints are actuated by the combination of knee motors and the quadriceps. In order to demonstrate efficacy, the control approach was implemented on three paraplegic subjects with motor complete spinal cord injuries ranging from levels T6 to T10. Experimental data indicates that the cooperative control system provided consistent and repeatable gait motions and reduced the torque and power output required from the hip and knee motors of the exoskeleton compared to walking without FES.

1.2 Introduction

One of the most significant impairments resulting from paraplegia is the inability to stand and walk [32]. In addition to diminished mobility, spinal cord injury (SCI) and the inability to stand and walk can entail significant health implications, including loss of bone mineral content, pressure-induced skin problems, increased incidence of urinary tract infection, muscle spasticity, impaired lymphatic and vascular circulation, impaired digestive operation, and reduced respiratory and cardiovascular capacities [58]. In an effort to restore legged locomotion to individuals with paraplegia, a number of researchers have investigated the use of functional electrical stimulation (FES) to artificially elicit and control leg muscle contraction, thereby

utilizing the musculature and metabolic power supply of the paraplegic subject to generate legged locomotion. Some of the research efforts in this regard include [59-69]. In addition to providing power for locomotion, FES-aided gait has also been shown to provide a number of associated physiological benefits, some of which include increased muscle strength, increased bone density, decreased spasticity, and improved cardiovascular health [7, 33-38]. Despite this, FES-based systems entail a number of challenges; most notably, muscles are difficult to control, particularly in the absence of adequate sensory information, and muscle torque output tends to fatigue rapidly, as a byproduct of the synchronous activation and preferential recruitment of fast-twitch muscle fibers associated with FES.

In order to address these challenges, some researchers have developed hybrid systems, which combine FES with lower limb orthoses [70-77]. The orthoses described in these works vary widely, but generally incorporate some combination of joint and/or load sensing (e.g., joint angle sensing), joint coupling (e.g., via reciprocating gait orthoses), and controllable joint locking or braking (e.g., electrically-actuated knee locks). Such systems also commonly restrict non-essential degrees-of-freedom (DOFs) during standing and walking. As a result, these devices reduce the number of DOFs that require control and introduce control elements that improve control of movement. These systems do not provide motive power for locomotion, but rather rely on FES as the source of motive power. Relative to FES-only approaches, hybrid approaches have shown improved control of movement and reduced muscle fatigue (the former a result of sensing and/or controlled braking elements, the latter generally a result of using the orthosis to lock the knee joints during standing and stance).

Rather than utilize the metabolic power source provided by stimulated muscle, other researchers have developed powered lower limb exoskeletons to facilitate walking, which utilize external power (e.g., a battery pack) in combination with joint actuators to provide a source of motive power that actively generates leg joint movement. Some of the efforts in this regard include [39-48, 78, 79]. Powered exoskeletons avoid the controllability and fatigue issues associated with FES and (to a lesser extent) hybrid-FES approaches, but do not offer (to the same extent) several physiological benefits associated with FES, and similarly do not leverage the presence of the metabolic power supply.

In this paper, the authors combine the use of an externally powered lower limb exoskeleton with FES, in order to form a powered hybrid FES system. The intent of the system is to combine the power and movement control advantages of the powered lower limb exoskeleton with the physiological benefits provided by FES. The proposed system is of the same general class of systems as the hybrid FES systems previously cited (i.e., [70-77]), but incorporates two sources of motive power (metabolic and robotic), and therefore offers additional control authority with which to supplement the FES. Such an approach requires a control methodology that can effectively combine these dissimilar sources of motive power, which is the topic of this paper.

Some researchers have recently explored the notion of combining FES with powered exoskeleton systems for individuals with paraplegia, as described in [80, 81]. In [80], the authors describe a feasibility study combining quadriceps stimulation with a lower limb exoskeleton that includes hip and knee joint actuation. In that work, the authors manually tune a quadriceps stimulation pulse on a single healthy subject, and show that once appropriately tuned, the quadriceps stimulation decreased the torque required from the knee actuator to achieve similar joint angle tracking. In [81], the authors also describe a control method for combining FES with a powered knee joint, and implemented this method on five healthy subjects. In that work, the knee joint motor is controlled by a variable-stiffness controller, with the stiffness controlled as a function of the interaction torque between the user and the exoskeleton. Concurrently, the knee extensor muscle stimulation is controlled by a PID controller, and knee flexor muscle stimulation is controlled by an iterative learning controller.

In this paper, the authors describe a control method for the cooperative control of a powered exoskeleton and FES, and demonstrate its efficacy on three SCI subjects. The method takes a different approach than those previously cited, and in particular, combines high-bandwidth position feedback around the motor actuators with quasi-real-time torque feedback around muscle stimulation, in order to minimize the motor torque required for each successive stride. The authors apply the cooperative control approach on an exoskeleton with powered hip and knee joints, in combination with a four-channel FES system that stimulates the quadriceps and hamstrings muscle groups of each leg, such that the quadriceps are used to provide extension at

the knee during swing, and the hamstrings are used to apply extension at the hip during stance. In order to demonstrate the efficacy of the approach, the cooperative controller was evaluated on three subjects with thoracic-level motor-complete SCI during level walking. Data is presented comparing the joint trajectories and exoskeleton torque and power requirements with and without muscle stimulation.

1.3 Cooperative Controller

1.3.1 Overview

The goals of the cooperative controller are (1) to ensure consistent and repeatable gait motions in the presence of time-varying and poorly-modeled muscle response, and (2) to maximize the constructive contribution of muscle torque in providing motive power for movement. Since muscle torque output resulting from electrical stimulation is known to have highly time-varying behavior, and since real-time sensing of muscle torque is not generally available, the authors do not attempt to use real-time control of the muscle to achieve motion tracking. Rather, the control architecture achieves the aforementioned objectives by combining a high-bandwidth, high-control-authority feedback loop that relies on the motors to ensure consistent joint trajectory tracking, with a low-bandwidth, low-accuracy component that adaptively (on a step-by-step basis) shapes the nature of the muscle stimulation in an effort to create a constructive influence on the motor control loop that effectively reduces the torque required from the motors. In this manner, the torque contribution from the muscles can be viewed as a disturbance to the exoskeleton joint trajectory control loop, and the purpose of the stimulation controller is to create a joint torque "disturbance" that energetically assists the closed-loop joint trajectory controllers. The general structure of the joint-level control architecture is illustrated in Figure 4.1. Note that muscle torque $\tilde{\tau}_m$ is unidirectional, and that the validity of the torque summing junction in the joint angle feedback loop implicitly assumes an appropriate degree of backdrivability in the joint actuators.

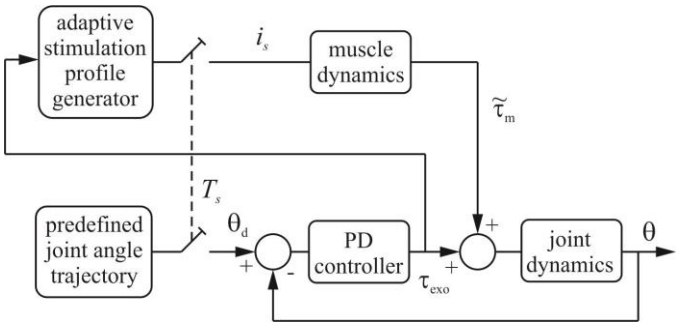

Figure 4.1. Joint-level control architecture of the cooperative controller combining high-bandwidth position feedback around the motors with quasi-real-time torque feedback around muscle stimulation. The motor control loop ensures consistent joint trajectory tracking, while the stimulation profile generator adaptively (on a step-by-step basis) shapes the nature of the muscle stimulation to create constructive muscle torque. Note that T_s goes high when a step is triggered, and remains high for the duration of the step.

The control structure shown in Figure 4.1 incorporates two feedback loops. The first is the motor control loop, which is a PD control loop that uses joint angle feedback (in real time) to control the output of the joint motors to track the desired joint trajectories. The second feedback control loop is the muscle control loop. The muscle control loop does not occur in real time, but rather occurs on a step-by-step basis (as described below), and at each successive step utilizes the motor torque profiles measured from preceding steps to adapt the shape of the muscle stimulation profile in an effort to reduce the motor torque required for the subsequent step. Each time a subsequent step is triggered (indicated by the T_s switch in Figure 4.1), the control loop executes a predetermined joint angle trajectory and utilizes a stimulation profile that was adaptively determined immediately following the end of the preceding step. As such, the stimulation profile does not change within a given step, but rather is updated between successive steps.

1.3.2 Measurement of Estimated Muscle Torque

As previously stated, the stimulation controller adapts the stimulation profile based on the motor torque profiles observed during previous steps. Specifically, the exoskeleton is capable of measuring motor torque but is unable to directly measure the torque contribution from the stimulated muscle. Direct measurement of muscle torque would require instrumentation between the muscle and joint (e.g., in the respective muscle tendon), which is not practical for the

proposed application. Recognizing that gait is a periodic event, rather than monitor muscle torque contribution in real time (or use model-based methods such as a disturbance observer), the muscle torques can be monitored in quasi-real time by comparing measured joint motor torques during gait cycles with and without FES, assuming that the differences in torques between respective gait cycles are primarily attributable to stimulated muscle contraction. Specifically, the control architecture assumes a quasi-stationary periodic system, and in particular assumes that the joint angle trajectories and the joint dynamics remain essentially invariant between steps. Note that this assumption does not assume an invariant muscle dynamics (i.e., dynamics between stimulation and muscle torque), which in general will vary considerably over time.

Given the quasi-stationary periodic assumption, a baseline measurement of the requisite motor torques can be recorded by initially walking without stimulation, and an estimate of muscle contribution in subsequent gait cycles can be provided by subtracting motor torque contribution during cycles with FES from the baseline. The method of muscle torque measurement is thus as follows. The controller initializes by taking several steps without using muscle stimulation. A nominal torque profile τ_n is established by averaging the motor torque required to track the desired joint angle profile over these several steps. Once this nominal torque profile is established, the portion of that profile corresponding to the stimulated muscle group (the positive or negative portion of the torque, depending on whether the muscle group is a flexor or extensor group) is regarded as the torque reference τ_r for that muscle group. Ideally, a stimulation profile would be generated such that the stimulated muscle provides a muscle torque contribution that exactly matches the torque reference (in which case the motors would not contribute any torque during the corresponding portion of that movement). Following establishment of the nominal torque profile, the torque contribution from the stimulated muscle can be estimated by subtracting the motor torque measured during a step with FES from the nominal torque profile:

$$\tau_m = \tau_n - \tau_{exoFES} \tag{1}$$

where τ_m is the estimated muscle torque profile for a given step, and τ_{exoFES} is the motor torque measured during a step with FES. Note that in the implementation described here, all torque

profiles are established as a filtered five-step average, as described in more detail in the implementation section. Note also in Figure 4.1 that $\tilde{\tau}_m$ is used to denote the actual muscle torque, which is not (in this system) known or directly measurable. Following each step, the torque reference profile τ_r is compared to the estimated muscle torque profile τ_m , and the difference between the two profiles is used to adaptively shape the muscle stimulation profile as subsequently described.

1.3.3 Adaptive Shaping of Stimulation Profile

Figure 4.2 describes the nature of the adaptive stimulation profile generation. Since the torque references for all stimulated muscle groups considered here have an essentially pulse-like character (see results section), and since stimulation is regarded here as a low-accuracy, low-bandwidth component of control, the authors restrict the envelope of the stimulation profile to be in the form of a pulse. Note that this pulse is the envelope of the actual stimulation waveform (see Figure 4.2). Note also that although a rectangular pulse profile (controlled in an on-off manner) was selected for the work presented here, the general adaptation method could be similarly implemented with a more complex stimulation profile shape, if desired.

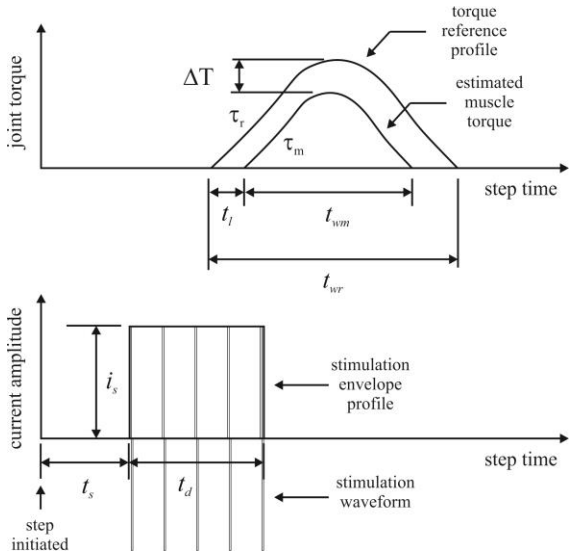

Figure 4.2. Parameters involved in adaptive stimulation profile shaping. The stimulation envelope profile, which is expressed using the pulse start time t_s, pulse duration t_d, and pulse amplitude i_s, is adaptively shaped based on feature differences between the torque reference τ_r and the estimated muscle torque τ_m.

With the assumption of a rectangular pulse profile, the stimulation profile associated with each step can be defined by three parameters, which are the pulse start time t_s (relative to the step start time), the pulse duration t_d, and the pulse amplitude i_s (i.e., current amplitude of the stimulation waveform), all of which are identified in Figure 4.2. The stimulation profile is adaptively shaped based on feature differences between τ_r and τ_m as described in Figure 4.2. Specifically, the feature differences between the torque profiles are described by the muscle torque lag time t_l, which is the period of time by which τ_m lags τ_r; the pulse width difference given by:

$$\Delta t_w = t_{wr} - t_{wm} \tag{2}$$

where t_{wr} and t_{wm} are the respective pulse widths of τ_r and τ_m; and the difference between the reference and estimated muscle torque amplitude given by ΔT (which is the error in torque amplitude). Given an initial set of values describing the pulse profile, the parameters describing the stimulation profile are adaptively updated after each step as follows. The pulse start time for the next step is given by:

$$t_{s(k)} = t_{s(k-1)} - t_{l(k-1)} \tag{3}$$

where $t_{s(k)}$ is the start time of the stimulation pulse for the next step; $t_{s(k-1)}$ is the start time of the stimulation pulse in the preceding step; and $t_{l(k-1)}$ is the measured muscle torque lag time (from the preceding step). The pulse duration of the next step is given by:

$$t_{d(k)} = t_{d(k-1)} + D\,\mathrm{sgn}(\Delta t_{w(k-1)}) \tag{4}$$

where $t_{d(k)}$ is the pulse duration of the stimulation pulse for the next step; $t_{d(k-1)}$ is the pulse duration of the stimulation pulse in the preceding step; $\Delta t_{w(k-1)}$ is the measured pulse width difference (from the preceding step); and D is a predetermined increment (set to an increment

that would add or remove one stimulation pulse for the implementation here). Note that, unlike the start time, the pulse duration is quantized by the period of the stimulation waveform. For example, for a stimulation frequency of 40 Hz, the minimum increment in duration would be 25 ms. As such, this adaptive component is subject to the quantization imposed by the selected frequency of stimulation. Finally, the amplitude of the stimulation profile, which corresponds to the current amplitude of each individual stimulation pulse, is adaptively incremented or decremented as follows:

$$i_{s(k)} = i_{s(k-1)} + I\,\mathrm{sgn}(\Delta T_{(k-1)}) \tag{5}$$

where $i_{s(k)}$ is the pulse amplitude of the stimulation pulse for the next step; $i_{s(k-1)}$ is the pulse amplitude of the stimulation pulse in the preceding step; $\Delta T_{(k-1)}$ is the measured error in torque amplitude (from the preceding step); and I is a predetermined increment (2.5 mA for the implementation here, as discussed subsequently). Hysteresis elements were added to (4) and (5) in order to prevent chatter as the stimulation duration and amplitude converge to steady-state values.

Therefore, each parameter defining the stimulation pulse profile is adaptively updated at discrete-time intervals corresponding to each subsequent step time. The start time and pulse duration stimulation profile parameters are simply shifts of the pulse start and end times, relative to the start time of the step, to best align the muscle torque pulse with the pulse reference, and where the end time (as determined by the pulse duration) is subject to the quantization effects of stimulation. The pulse amplitude is essentially controlled by a slew-rate-limited proportional control law, updated at a discrete time step that corresponds to each subsequent stride. Note finally that all stimulation pulse parameters are bounded within appropriate limits.

1.3.4 Muscle Fatigue Detection

In order to prevent overstimulation of fatigued or non-responsive muscles, the controller monitors the torque output of each muscle and selectively stops stimulating any individual

muscle group that it deems severely fatigued. Severe muscle fatigue is defined for purposes of this controller as a muscle gain (i.e., joint torque output relative to stimulation amplitude input) one third the maximum observed muscle gain. That is, for a given input, once the muscle is only able to generate one third the output torque it was previously able to generate, it is considered substantially fatigued and thus considered essentially unresponsive to the stimulation controller. If muscle fatigue is detected for a given muscle over five consecutive steps, the controller stops stimulating the fatigued muscle for a period of two minutes to allow time for recovery.

1.4 Experimental Implementation

The control approach described in the previous section was implemented on a powered lower limb exoskeleton supplemented by FES, and its ability to provide effective control was assessed on three subjects with thoracic-level motor-complete SCI. Specifically, the exoskeleton included powered actuation at both hip and knee joints, and the FES system included four channels of stimulation, which were the quadriceps and hamstrings muscle groups of each leg. The quadriceps consists of four heads: rectus femoris, vastus lateralis, vastus intermedius and vastus medialis. The rectus femoris is a biarticular muscle spanning both the hip and knee joints with its two actions being hip flexion and knee extension. The other three act on the knee joint only with their main action being knee extension [82]. Overall, contraction of the quadriceps muscle group as a whole generates an extension torque at the knee. The hamstrings consist of three heads: semitendinosus, semimembranosus and the long head of biceps femoris. All three are biarticular muscles spanning both the hip and knee joints with their main actions being knee flexion and hip extension [82]. When the knee joint is immobilized, as it is in the stance phase in this application (by the normally-locked knee joints of the exoskeleton), hamstring contraction generates an extension torque at the hip. As such, four cooperative control loops were included in the hybrid system, two consisting of hip motors supplemented by hamstring stimulation (used during the stance phase of walking), and two consisting of knee motors supplemented by quadriceps stimulation (used during the swing phase of walking).

1.4.1 Lower Limb Exoskeleton

The Vanderbilt lower limb exoskeleton, shown in Figure 4.3, is a powered exoskeleton described in [46, 47] for gait restoration in persons with paraplegia. It includes electric motors at both hip and knee joints, in addition to a four-channel muscle stimulator, used here for stimulation of the quadriceps and hamstrings muscle groups. In addition to the motors, the knee joints additionally incorporate normally-locked brakes, which were implemented primarily as a safety measure, to prevent knee buckling in the event of a power failure. The device does not have foot and ankle sections but rather is used with standard ankle foot orthoses (AFOs). The total exoskeleton mass is 12 kg (26.5 lb) including the 29.6 V, 3.9 A·hr lithium polymer battery.

Figure 4.3. Vanderbilt lower limb exoskeleton

The exoskeleton is controlled via a pair of embedded electronic systems, one located within each thigh segment, each containing an 80 MHz PIC32 microcontroller, in addition to a pair of switching servoamplifiers for the knee and hip motors of the respective leg. The electronics board in each leg additionally incorporates a two-channel electrical stimulator, which provides computer-controllable electric stimulation for the quadriceps and hamstrings muscle groups of each leg. Each stimulator produces two independent channels of current-controlled symmetrical biphasic stimulation pulses. The pulse width, current amplitude, and pulse frequency of each biphasic stimulation channel are controllable via the microcontroller. One of the two exoskeleton

control boards, along with the plug-in electric stimulator that is typically mounted on it, is shown in Figure 4.4. In order to facilitate prototyping and implementation of the cooperative controller, the embedded system in the exoskeleton is interfaced with MATLAB Real-Time Workshop via a CAN tether, such that all sensor inputs and control outputs of the exoskeleton, including stimulation channels, are assessable and controllable, respectively, from a laptop computer.

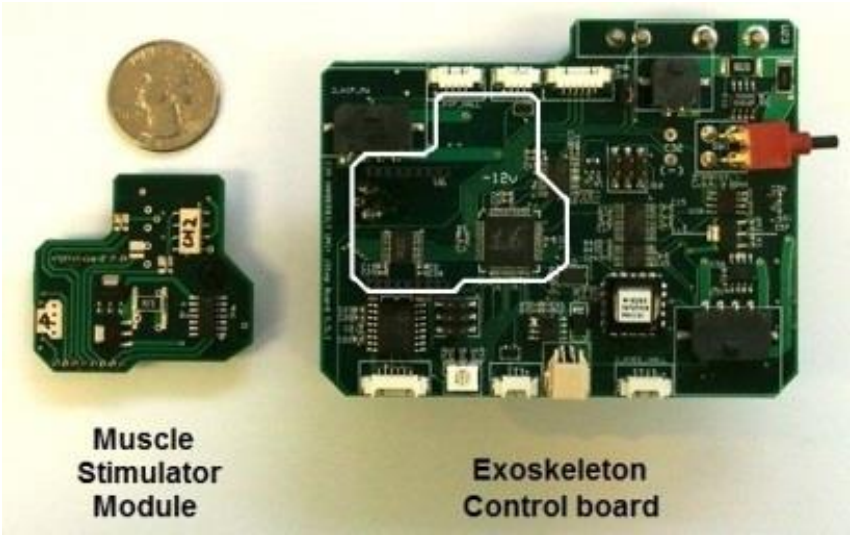

Figure 4.4. Exoskeleton control board, shown with muscle stimulator module (which plugs into the control board within the outline shown)

1.4.2 Controller Implementation

The four cooperatively actuated muscle/motor pairs are the left and right quadriceps and knee motor combination (used during swing), and the hamstrings and hip motor combination (used during stance). As such, the control structure shown in Figure 4.1 was implemented at each of these four joints. The inputs to these joint-level cooperative controllers are governed by a finite state machine (FSM), which is described in detail in [47]. For purposes of walking, the FSM is described by four essential states, which are right step (state 1), double-support with right foot forward (state 2), left step (state 3), and double-support with left foot forward (state 4), as illustrated in Figure 4.5. During normal walking, the state machine moves sequentially through these states in a repeating fashion, as illustrated in Figure 4.6. As described in [47], each successive step is initiated by a shift in the location of the projection of the user's estimated

center of pressure (CoP) along the ground in the sagittal plane, relative to the user's forward foot (i.e., when the CoP projection shifts forward to a sufficient extent, the subsequent step will be triggered). When a right step is triggered (i.e., when state 1 is entered), predetermined joint angle profiles (given in [47]) are used as input in the control loops for the right knee and hip control loops (for swing), and for the left hip control loop (for stance), while the left knee is locked. Additionally, the most recent right quadriceps stimulation profile is used as input to the right knee control loop, and the most recent left hamstrings stimulation profile is used as input to the left hip control loop. Once the right step has ended (i.e., the joint trajectories are complete), the FSM enters state 2, and motors alone are used to hold the double-support posture. When a left step is triggered based on the projected CoP (i.e., when state 3 is entered), the predetermined joint angle profiles (given in [47]) are used as input in the control loops for the left knee and hip control loops (for swing), and for the right hip control loop (for stance), while the right knee is locked. Additionally, the most recent left quadriceps stimulation profile is used as input to the left knee control loop, and the most recent right hamstrings stimulation profile is used as input to the right hip control loop. Note that in the states for which a given joint does not utilize stimulation, the control structure remains as shown in Figure 4.1, with the stimulation profile set to zero (i.e., the controller simply tracks a given trajectory with motors only).

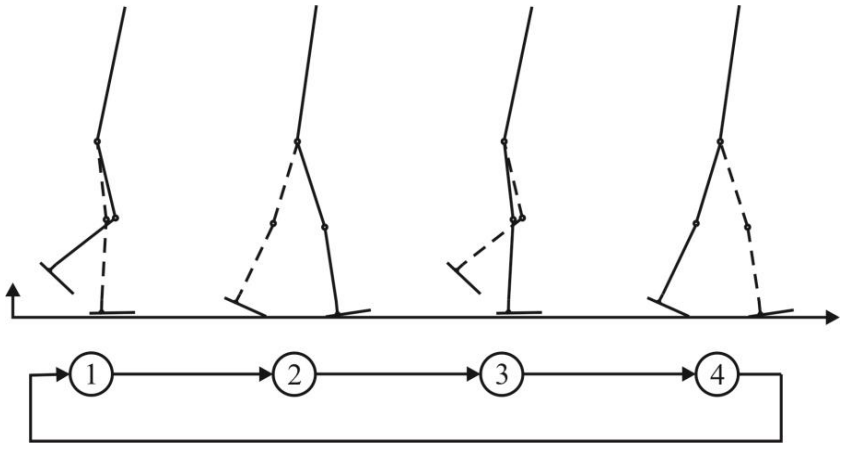

Figure 4.5. The finite state machine with four states involved in walking: right step (state 1), double-support with right foot forward (state 2), left step (state 3), and double-support with left foot forward (state 4).

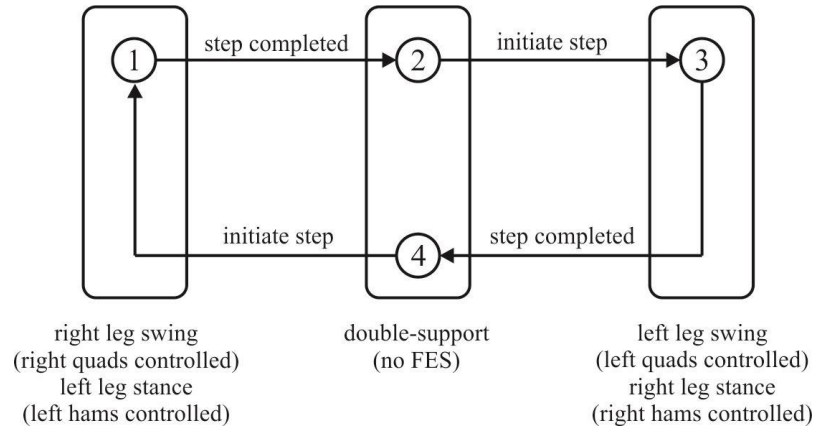

Figure 4.6. The four states involved in walking and the muscles stimulated

As previously described, upon initiation of walking, the initial five steps (of each cooperatively-controlled joint) occurred without stimulation, and the measured motor torque profile from each step was averaged to establish a nominal torque profile. Note that the five-step averaging was implemented to account for slight variations in motor torque between each step (which was observed despite the assumption of a stationary process), and to prevent substantial deviations in the estimated torque profile from occasional atypical steps. A muscle torque reference profile was created from the nominal torque profile by considering only the direction of torque corresponding to the stimulated muscle group. For the experiments described here, both muscle groups generated extension torques about their respective joints. As such, only the positive portions of the nominal torque profiles were used to establish the torque reference for each muscle group. Once this torque reference was established (i.e., after the first five steps, for a given leg), the control parameters describing the stimulation pulse envelope were initialized as follows. The pulse start time was set to occur 200 ms prior to the onset of the torque reference pulse; the pulse duration was set to the same duration as the torque reference pulse; and the pulse amplitude was set to 45 mA.

The control parameters describing the stimulation pulse envelope were subsequently adapted every subsequent step, based on the adaptation method previously described. For the experiments presented here, motor torque measurements were median-filtered with a window size of 75 ms (i.e., 15 samples at 200 Hz), low-pass filtered with a cutoff frequency of 30 Hz, and running averaged over the preceding five steps. The difference between the nominal torque profile and

measured torque during stimulation was considered the estimated muscle torque (equation 1). The control parameters describing the stimulation pulse envelope were then adapted, based on the previously described adaptation rules (equations 3-5), using the differences between the estimated muscle torque profile (from the previous step) and the torque reference (established from the first five steps), in order minimize the differences between the two. For the control implementation described here, the step-wise increment (i.e., slew rate) for current amplitude adaptation (equation 5) was set to 2.5 mA. The respective step sizes (for stimulation duration and amplitude) serve as the gains of the discrete-time (i.e., step-by-step) adaptive controller. Maintaining low adaptation gains enhances the stability of adaptation, at the cost of limiting responsiveness (e.g., requiring four steps to adapt the stimulation amplitude by 10 mA). Although these gains are low, they provide sufficient responsiveness for this application, since the intent of the control system is to provide hundreds of steps of walking per session.

1.4.3 Experimental Demonstration

The cooperative controller was implemented on three subjects with motor-complete spinal cord injuries ranging from levels T6 to T10. Two subjects had motor and sensory complete paraplegia (American Spinal Injury Association Impairment Scale, AIS, A classification), and one had motor-complete, sensory-incomplete paraplegia (AIS, B classification). The essential physical and injury characteristics of each subject are listed in Table 6. Subject 2 had prior experience with FES and was using it for quadriceps stimulation for a few hours a month at the time of this study. Subjects 1 and 3 had no prior experience with FES.

Table 6: Summary of Subject Profiles

	Subject 1	Subject 2	Subject 3
ASIA Impairment Scale	AIS A (Complete)	AIS A (Complete)	AIS B (Sensory Incomplete)
Injury Level	T8	T10	T6
Years since Injury	4	11	2
Gender	Male	Male	Male
Age	41	43	19
Height (m)	1.75	1.85	1.75
Weight (kg)	82	75	54

Commercially available surface electrodes were used to stimulate the muscles. For the quadriceps, electrodes were applied to the anterior thighs with the subjects sitting up. For the hamstrings, electrodes were applied to the posterior thighs with the subjects lying supine with the leg held in a position with the knee extended and hip flexed. Figure 4.7(a) indicates the location of the surface electrodes. Once the electrodes were applied, muscle contractions were visually confirmed before donning the exoskeleton. After donning the exoskeleton, the electrode leads were connected to the exoskeleton stimulator jacks. The stimulation waveforms consisted of biphasic waveforms with a 200 µs pulsewidth for each polarity of the biphasic wave, for a combined pulsewidth of 400 µs, and implemented with a pulse frequency of 50 Hz for the quadriceps and 25 Hz for the hamstrings. Note that the quadriceps groups were stimulated at 50 Hz (rather than 25) to increase the resolution of the stimulation pulse envelope in time (i.e., to provide a pulse envelope resolution of 20 ms in time rather than 40 ms).

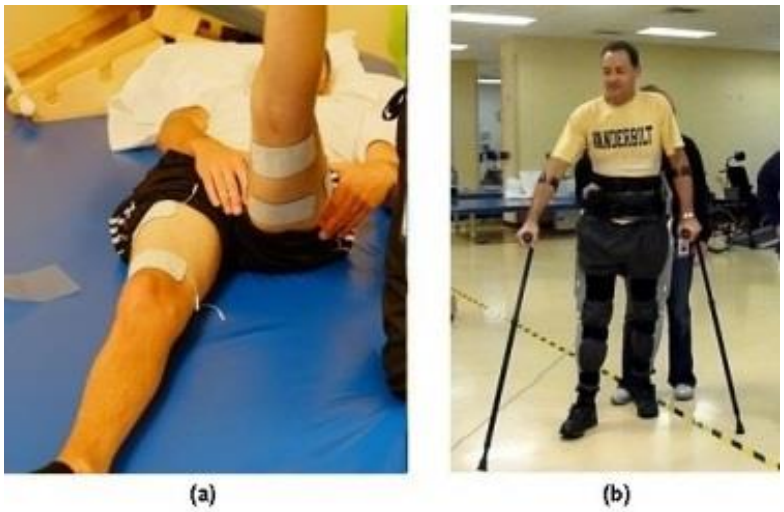

Figure 4.7. Experimental setup. (a) Surface electrodes placed over the quadriceps and hamstrings. (b) Subject walking with the exoskeleton.

Following donning of the system, subjects were instructed to walk continuously at a comfortable pace. Figure 4.7(b) shows a subject walking in the FES-assisted exoskeleton. The controller was initialized as described above. Each subject walked continuously on level ground for approximately ten minutes, approximately half while using FES, and half without, while data was continuously recorded regarding joint angles, motor torque, and stimulation levels. In terms of steps, Subject 1 took 140 steps with FES and 139 steps without FES for a total of 279 steps;

Subject 2 took 160 steps with FES and 164 steps without FES for a total of 324 steps; and Subject 3 took 99 steps with FES and 105 steps without FES for a total of 204 steps. In order to provide a high degree of uniformity between the conditions with and without FES, the system alternated continuously every ten steps between the controller without FES and the controller with FES. Note that system could only switch controllers during the double-support phases of gait (i.e., states 2 or 4). A video is included in the supplemental material showing one of the SCI subjects (Subject 2) walking with and without FES.

1.5 Results and Discussion

1.5.1 Reference Torques and Stimulation Profile Adaptation

Figures 4.8 and 4.9 show representative measured nominal and reference torques corresponding to walking (excerpted from data from Subject 2). Specifically, Figure 4.8(a) shows the nominal torque corresponding to the swing phase of the knee joint with stimulation, which is the total knee joint motor torque measured during the swing phase and averaged over five gait cycles without stimulation. Figure 4.8(b) is the positive portion of the nominal torque, which is the portion in which the torque is extending the knee, and thus the only portion during which the quadriceps group can contribute. Figures 4.9(a) and (b) show the same, but taken at the hip joint during the stance phase, and showing the portion of torque to which the hamstrings can contribute (which is most of the stance phase). Note that the stance and swing phases are both one second because when a step is triggered, each joint follows a predetermined trajectory, which (for the trajectory used for these experiments) occurs over one second for both the stance and swing sides. Double-support phase, which is not shown in the data, occurs for a duration determined by the subject (i.e., the duration of double support depends on the time for the subject to trigger the next step).

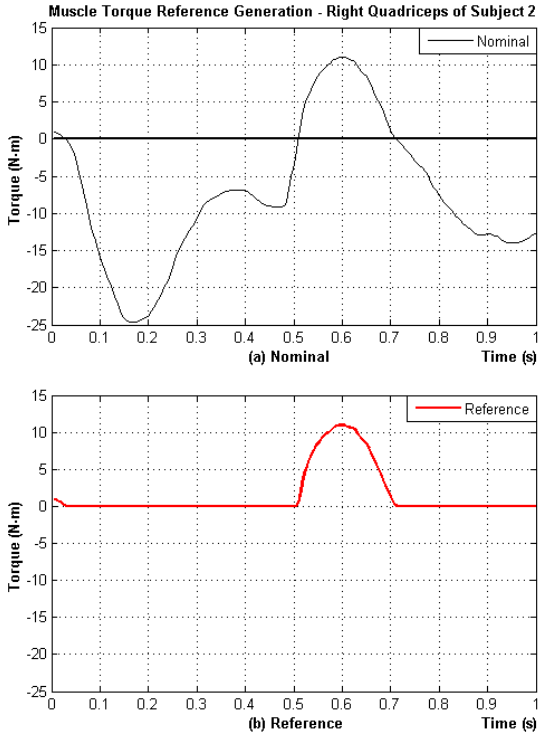

Figure 4.8. Quadriceps torque reference generation. (a) Nominal knee motor torque during swing. (b) Reference generated by removing flexion torques.

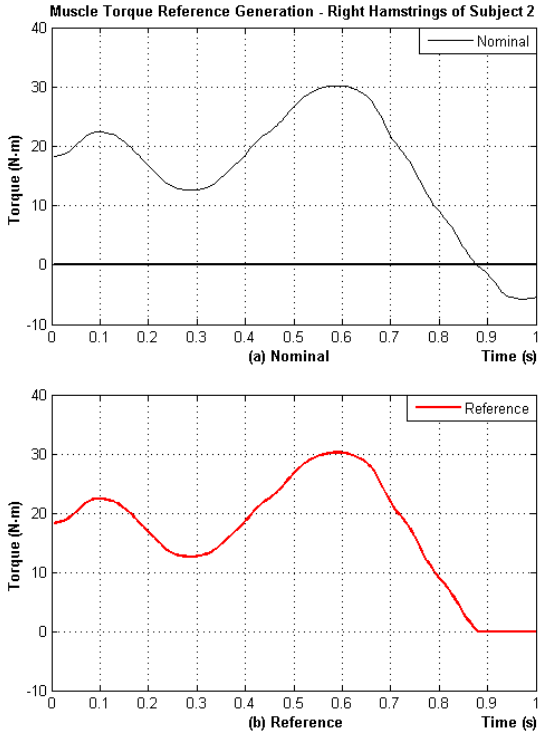

Figure 4.9. Hamstring torque reference generation. (a) Nominal hip motor torque during stance. (b) Reference generated by removing flexion torques.

Figures 4.10 and 4.11 show the stimulation pulse profile parameter adaptation for the quadriceps and hamstrings, respectively, for Subject 1 over the course of data collection with FES (i.e., over 140 steps). Note that the stimulation amplitude is shown as zero when walking without FES. As evidenced in the plots, the pulse parameters nominally converge, although vary somewhat about the nominal values, presumably due primarily to muscle fatigue. Also, one can observe in Figure 4.11 the two periods during which the controller observed severe muscle fatigue (as previously defined), and in response turned off muscle stimulation for two respective two-minute rest periods. As indicated in Figure 4.10, the quadriceps muscles did not exhibit severe fatigue during this data set.

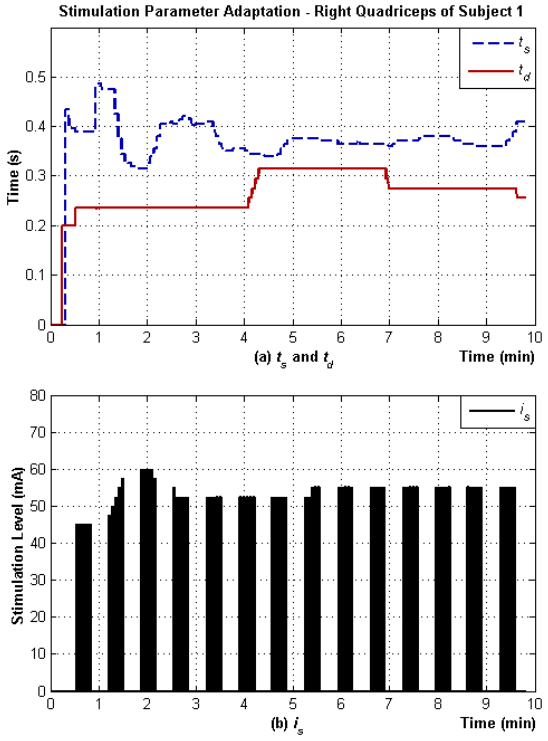

Figure 4.10. Stimulation parameter adaptation for right quadriceps of Subject 1 during 10 minutes of walking. (a) Stimulation start time t_s (dashed line) and duration t_d (solid line). (b) Stimulation level i_s (solid bar).

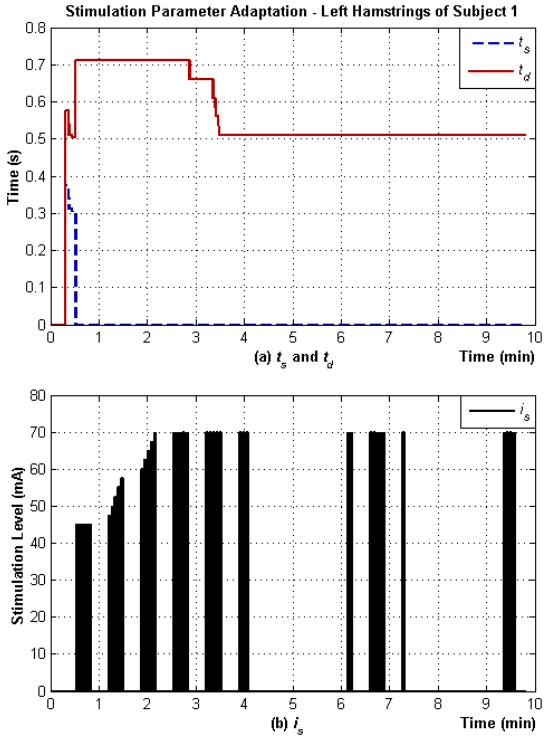

Figure 4.11. Stimulation parameter adaptation for left hamstrings of Subject 1 during 10 minutes of walking. (a) Stimulation start time t_s (dashed line) and duration t_d (solid line). (b) Stimulation level i_s (solid bar).

1.5.2 Joint Angle Trajectories

Figure 4.12 shows knee and hip joint angle trajectories during controller states 1 and 3 (i.e., during a step) for all steps taken by each subject, both with and without FES. Specifically, the plots show the average knee joint angles during the swing phase and the hip joint angles during the stance phase for steps taken with and without FES for each subject (along with plus and minus one standard deviation in the thin lines). Consistent hip and knee joint motions, as indicated by the data, support the (previously stated) claim that the exoskeleton is able to ensure consistent, reliable, repeatable motion in the presence of (quadriceps and hamstring) muscle stimulation. Consistent gait motions can also be observed in the included supplemental video, which shows one of the subjects walking with and without FES.

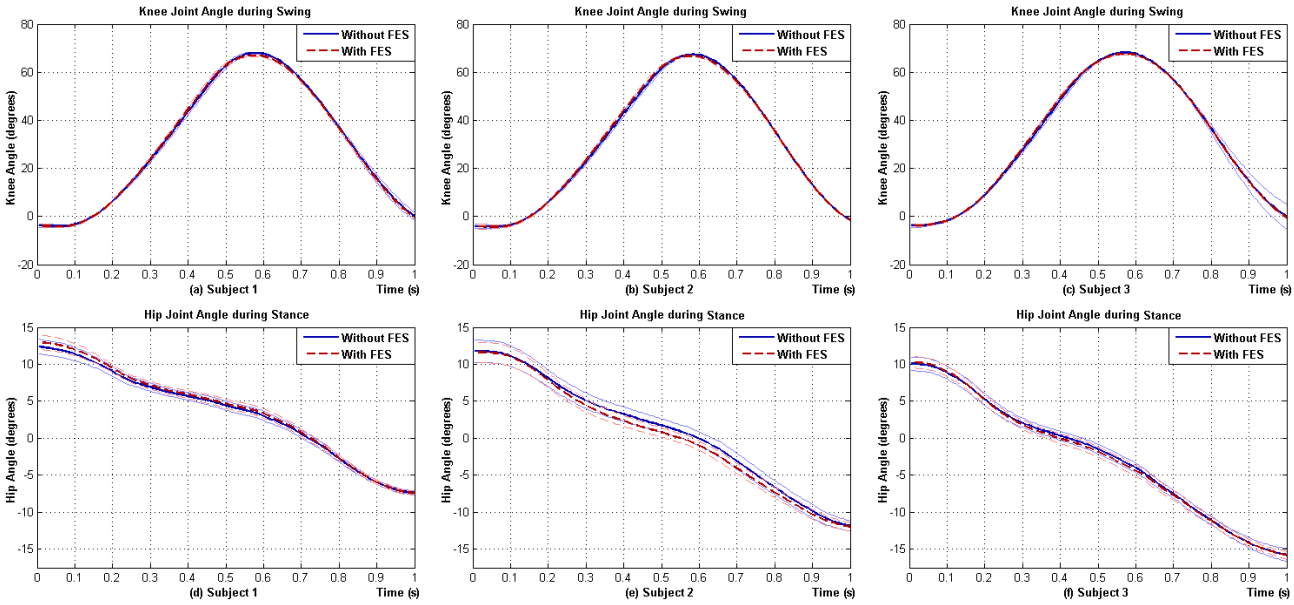

Figure 4.12. Knee joint trajectories during swing (a, b, and c) and hip joint trajectories during stance (d, e, and f) without FES (solid lines) and with FES (dashed lines) for three subjects. Thick lines are joint trajectories averaged over all steps. Thin lines indicate one standard deviation.

1.5.3 Muscle Torque and Power Contributions

1) Quadriceps

In all three subjects, the knee joint torque and power output required from the motor during the swing phase was lower with FES (i.e., quadriceps stimulation). Figure 4.13 shows the average knee joint power and motor torque with and without FES. Specifically, Figure 4.13 shows the average motor torque measured at the knee joints while walking with and without FES, along with plus and minus a standard deviation for each. On average, the torque contribution from the quadriceps ranged from 18% to 29% during the entire swing phase, for an average of 21% across all three subjects (Table 7). Note that the quadriceps is only able to provide a torque in extension (positive in the figure), and note also that the quadriceps on average provides the majority of the torque in the interval in which it is able to contribute (approximately 0.5 s to 0.9 s for Subject 1, 0.5 s to 0.7 s for Subject 2, and 0.45 s to 0.65 s in Subject 3). During this interval, the quadriceps contributed between 69% and 84% of the torque required for knee extension (with the remainder provided by the motors), for an average of 79% across all three subjects (Table 8). Figure 4.13 also shows the average motor power measured at the knee joints while walking with and without

FES, along with plus and minus a standard deviation for each. As seen in the figure, the average power was essentially unchanged in swing flexion (i.e., up to approximately 0.5 s) with FES but on average was substantially lower during swing extension. In particular, the stimulated quadriceps contributed between 12% and 24% of knee joint power during the entire swing phase for an average of 20% across all three subjects (Table 7). During the extension interval only, the quadriceps contributed between 61% and 93% of the power for an average of 80% across all three subjects (Table 8). The computed average torque and power contributions from the quadriceps for all three subjects, during the entire swing phase, and during the subset of the swing phase during which the quadriceps generated torque, are given in Tables 7 and 8.

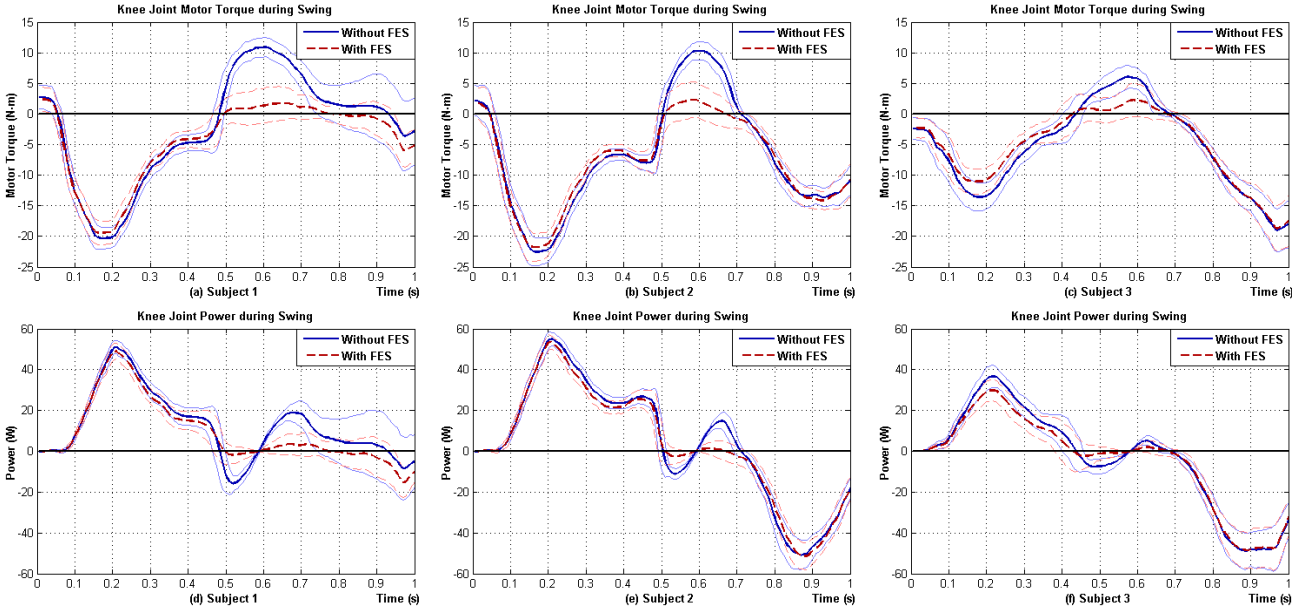

Figure 4.13. Exoskeleton knee motor torque (a, b, and c) and power (d, e, and f) during swing without FES (solid lines) and with FES (dashed lines) for three subjects. Positive values indicate extension torques, and negative values indicate flexion torques. Thick lines are averages of all steps. Thin lines indicate one standard deviation.

Table 7: Exoskeleton Knee Joint Motor Torque and Power With and Without FES

		Without FES	With FES	Muscle Contribution
Subject 1	Absolute Mean Knee Torque (SD)	7.2 N·m (2.6)	5.2 N·m (2.1)	29%
	Mean Positive Knee Power (SD)	14 W (6.4)	10 W (4.7)	24%
Subject 2	Absolute Mean Knee Torque (SD)	9.9 N·m (1.9)	8.4 N·m (2.1)	15%
	Mean Positive Knee Power (SD)	14 W (4.1)	12 W (4.3)	12%
Subject 3	Absolute Mean Knee Torque (SD)	7.2 N·m (2.0)	5.9 N·m (2.1)	18%
	Mean Positive Knee Power (SD)	7.3 W (2.0)	5.7 W (1.8)	23%
Three Subject Average	**Absolute Mean Knee Torque (SD)**	**8.1 N·m (1.6)**	**6.4 N·m (1.7)**	**21% (7.3)**
	Mean Positive Knee Power (SD)	**12 W (3.7)**	**9.4 W (3.4)**	**20% (6.3)**

Table 8: Exoskeleton Knee Joint Motor Torque and Power With and Without FES during Extension Torque Interval Only

		Without FES	With FES	Muscle Contribution
Subject 1	Absolute Mean Knee Torque (SD)	5.3 N·m (2.9)	0.84 N·m (2.2)	84%
	Mean Positive Knee Power (SD)	6.5 W (8.1)	0.96 W (5.2)	85%
Subject 2	Absolute Mean Knee Torque (SD)	6.9 N·m (1.7)	1.2 N·m (2.5)	82%
	Mean Positive Knee Power (SD)	5.0 W (3.2)	0.36 W (3.4)	93%
Subject 3	Absolute Mean Knee Torque (SD)	3.6 N·m (1.7)	1.1 N·m (2.1)	69%
	Mean Positive Knee Power (SD)	1.2 W (2.8)	0.45 W (3.0)	61%
Three Subject Average	**Absolute Mean Knee Torque (SD)**	**5.2 N·m (1.7)**	**1.1 N·m (0.19)**	**79% (8.0)**
	Mean Positive Knee Power (SD)	**4.2 W (2.8)**	**0.60 W (0.32)**	**80% (17)**

2) Hamstrings

The left hamstrings of Subject 1 were unresponsive to FES, presumably due to lower motor neuron damage associated with the spinal cord injury. As such, data from the left hamstrings of Subject 1 were not considered in the assessment of the cooperative control performance. All other muscle groups in all three subjects responded to FES and were included in the assessment of the controller performance. In all three subjects, the hip joint torque and power required from the motor during the stance phase was lower with FES (i.e., hamstring stimulation). The average hip joint torque and power with and without FES are shown in Figure 4.14. Specifically, Figure 4.14 shows the average motor torque measured at the hip joint while walking with and without FES, along with plus and minus a standard deviation for each. Based on the measured data, the hamstrings provided between 7.9% and 25% of the necessary hip torque during the entire stance phase, for an average of 18% across all three subjects (Table 9). Figure 4.14 also shows the average motor power measured at the hip joint while walking with and without FES, along with plus and minus a standard deviation for each. The hamstrings contributed between 7.5% and 31% of the hip joint power to the entire stance phase of gait, for an average of 20% across all three subjects (Table 9). The average torque and power contributions from the hamstrings for all three subjects during the entire stance phase are given in Table 9. Note that regarding the quadriceps and hamstrings contributions, with regular use of the exoskeleton (with FES), one would expect the results to show improved muscle strength and resistance to fatigue (see, for example, [14]).

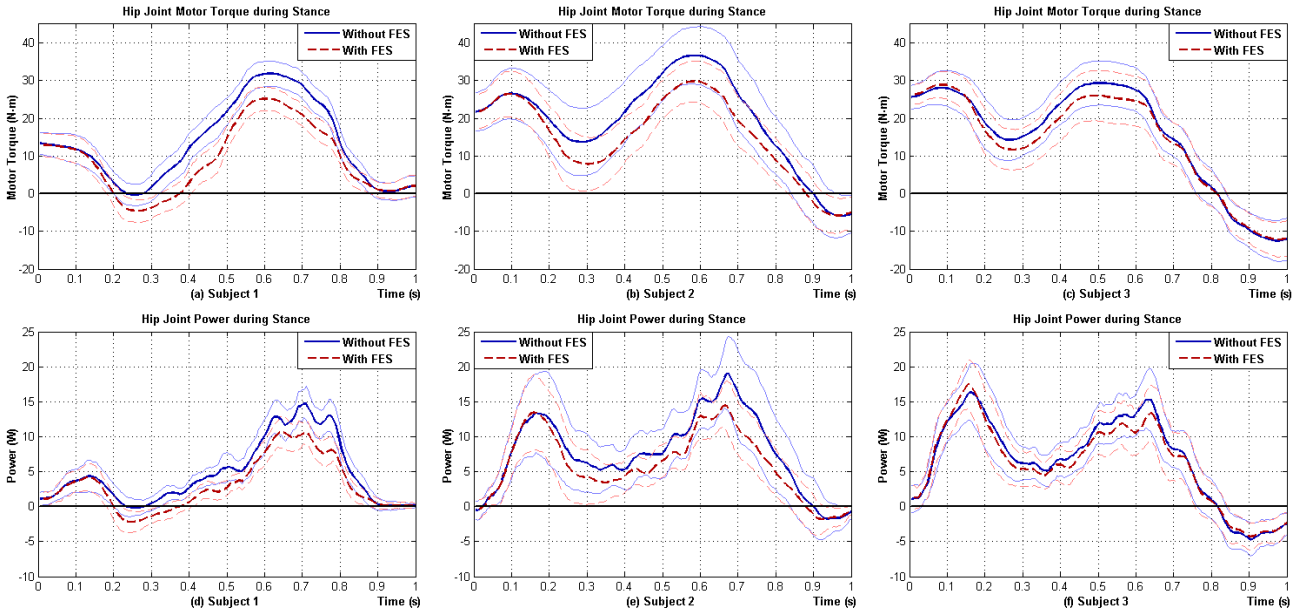

Figure 4.14. Exoskeleton hip motor torque (a, b, and c) and power (d, e, and f) during stance without FES (solid lines) and with FES (dashed lines) for three subjects. Positive values indicate extension torques, and negative values indicate flexion torques. Thick lines are averages of all steps. Thin lines indicate one standard deviation.

Table 9: Exoskeleton Hip Joint Motor Torque and Power With and Without FES

		Without FES	With FES	Muscle Contribution
Subject 1	Absolute Mean Hip Torque (SD)	13 N·m (3.3)	10 N·m (3.0)	25%
	Mean Positive Hip Power (SD)	4.7 W (1.5)	3.3 W (1.3)	31%
Subject 2	Absolute Mean Hip Torque (SD)	21 N·m (7.6)	16 N·m (5.9)	20%
	Mean Positive Hip Power (SD)	7.9 W (3.9)	6.2 W (3.0)	22%
Subject 3	Absolute Mean Hip Torque (SD)	19 N·m (5.2)	17 N·m (5.3)	7.9%
	Mean Positive Hip Power (SD)	7.3 W (2.9)	6.7 W (2.8)	7.5%
Three Subject Average	**Absolute Mean Hip Torque (SD)**	**18 N·m (3.7)**	**15 N·m (4.0)**	**18% (9.0)**
	Mean Positive Hip Power (SD)	**6.6 W (1.7)**	**5.4 W (1.9)**	**20% (12)**

3) Variability in Muscle Response

The controller was able to generate good muscle torque tracking in the presence of variable muscle behavior, as illustrated by Figure 4.15. Specifically, Figure 4.15 shows the average stimulation profile for the quadriceps, the torque reference profile, and the estimated muscle torque profile for the quadriceps stimulation of the right quadriceps of Subject 1 (Figure 4.15(a)), the left quadriceps of Subject 2 (Figure 4.15(b)), and the left quadriceps of Subject 3 (Figure 4.15(c)) during ten minutes of walking. Although all three stimulation profiles resulted in similar torque reference tracking, the respective pulse profiles were substantially different. Specifically, the left quadriceps of Subject 2 required shorter stimulation duration (60 ms vs. 260 ms and 280 ms for the other two), while achieving similar output duration. The left quadriceps of Subject 3 required higher stimulation amplitude, even though the torque output was lower (approximately 4.5 N·m vs. 9.5 N·m for the other two). The muscles also exhibited substantially different dynamics between the start of the pulse and onset of torque, ranging from 75 ms to 200 ms. Note that the stimulation profiles shown in Figure 4.15 are averages of multiple steps, and that muscle behavior varied over time within each subject as well (e.g., the stimulation pulse start time, duration, and amplitude shown in Figure 4.15(a) are averages of Figure 4.10).

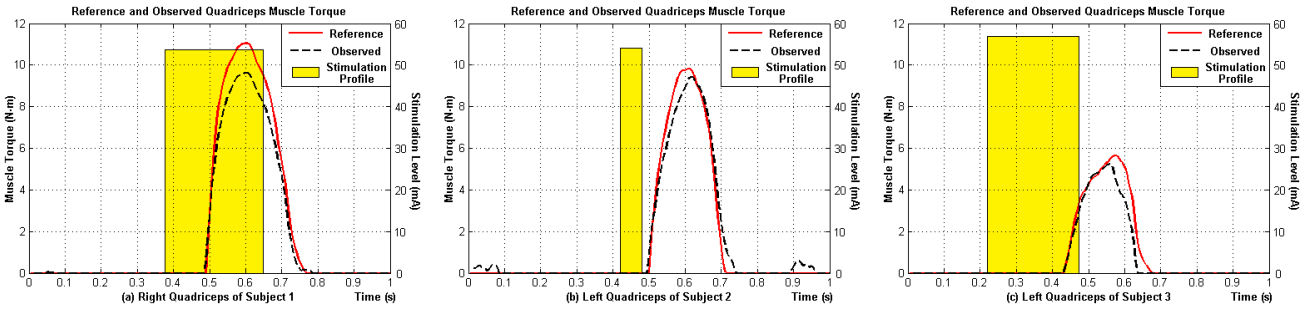

Figure 4.15. Variability in muscle response to FES. Stimulation envelope profile (filled rectangles), reference (solid lines) and observed (dashed lines) muscle torque for (a) right quadriceps of Subject 1, (b) left quadriceps of Subject 2, and (c) left quadriceps of Subject 3.

1.5.4 Feasibility of Hybrid Approach and Future Direction

The overarching goal of this study is to validate the feasibility of the hybrid control method that combines FES with a powered exoskeleton, which is expected to enhance physiological benefits

and concurrently minimize electrical power consumption. This study has shown that (1) the hybrid approach is technically feasible, (2) it is capable of providing consistent and repeatable gait motions, and (3) the muscle contribution reduces the torque and power required from the device. However, regarding physiological benefits of FES, a clinical trial with predefined endpoints and additional subjects for statistical power will be necessary in order to characterize the extent of health benefit resulting from the hybrid control approach.

1.6 Conclusion

The authors have presented a control approach that enables the cooperative control of a powered lower limb exoskeleton in combination with FES. The intent of the hybrid system is to provide the physiological benefits associated with FES, with the reliability and control benefits associated with the exoskeleton. The control approach treats the muscle stimulation as a disturbance to a high-bandwidth motor control loop, and incorporates a step-wise adaptation that shapes the stimulation profile based on the torque measurement from previous steps to shape the muscle "disturbance" in such a way that minimizes the required motor torque. Experimental results from testing the cooperative control system on three motor-complete thoracic-level paraplegic subjects indicated highly consistent hip and knee movement; the ability of the controller to actively adapt the muscle stimulation despite substantial variability in muscle dynamics, both within and between subjects; and the effective reduction of motor torque and power as a result of muscle stimulation.

1.7 Acknowledgment

This work was funded by the National Institutes of Health, grant no. R01HD059832. The authors gratefully acknowledge this support. The authors would also like to thank C. Hartigan, MPT, and S. Hawes, MPT for their contributions to the clinical portions of this work.

2. Addendum to Manuscript 3: Multichannel Biphasic Signal Generator Circuit

The muscle stimulator used in this work was designed and built in-house so that it can be embedded into the system both physically and for control purposes. It is controlled by the microprocessors in the exoskeleton, and its design incorporates novel features that allow it to generate multiple channels of current-controlled biphasic stimulation waves from a single source, thus reducing the number of components and the physical footprint of the circuit board. A provisional patent application has been filed based on the circuit design.

2.1 Hybrid H-bridge

In order to produce biphasic stimulation waves (i.e. to command current in both directions), the circuit uses four transistors in an H-bridge configuration with a transformer in the middle of the bridge. Figure 4.16 shows the H-bridge design. Closing (i.e. activating) transistors H1 and L2 results in current flowing through the transformer from left to right. Opening (i.e. deactivating) transistors H1 and L2, and closing transistors H2 and L1 reverses the direction of the current (so that current flows from right to left across the transformer).

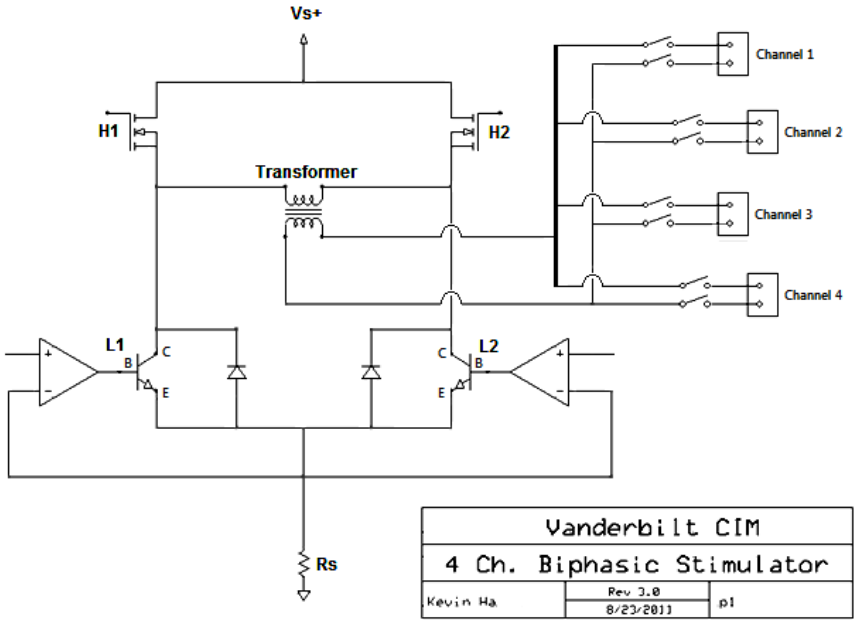

Figure 4.16. Hybrid H-bridge design

The H-bridge consists of two different types of transistors (thus the name hybrid H-bridge). Metal–oxide–semiconductor field-effect transistors (MOSFETs) are used as high-side transistors H1 and H2, and they act as on-off valves. In order to control the amount of current flowing through the transformer, bipolar junction transistors (BJTs) are used for transistors L1 and L2. Used in conjunction with a sense resistor, Rs, the low-side BJTs act as valves that control the amount of current that flow through the transformer. Figure 4.17 shows a biphasic stimulation pulse generated from the hybrid H-bridge.

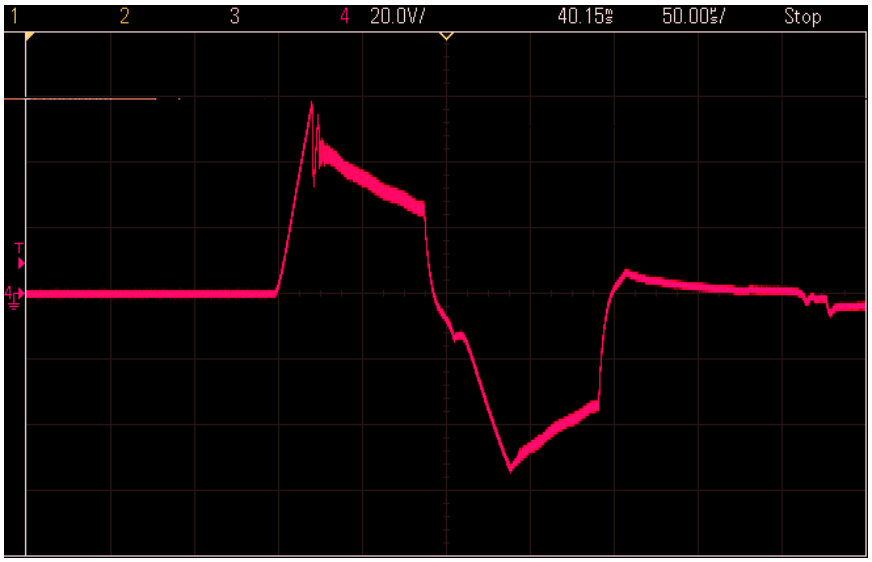

Figure 4.17. A biphasic stimulation pulse generated from the hybrid H-bridge

2.2 Signal Multiplexer

The circuit design takes advantage of the fact that muscle stimulators have very low duty cycle (around 2 % to 4 %), so that it can produce multiple channels from a single H-bridge. The microcontroller sends commands to the transistors, so that the H-bridge produces multiple biphasic waves that are staggered in time, and the waves are routed to different channels using high-bandwidth relays (that are also microcontroller-controlled), as shown in Figure 4.16. The stimulation pulse profile (pulsewidth, pulse amplitude, and pulse frequency) can be controlled independently for each channel. Figure 4.18 shows four channels of stimulation waves of varying pulse amplitude and frequencies generated from a single H-bridge source.

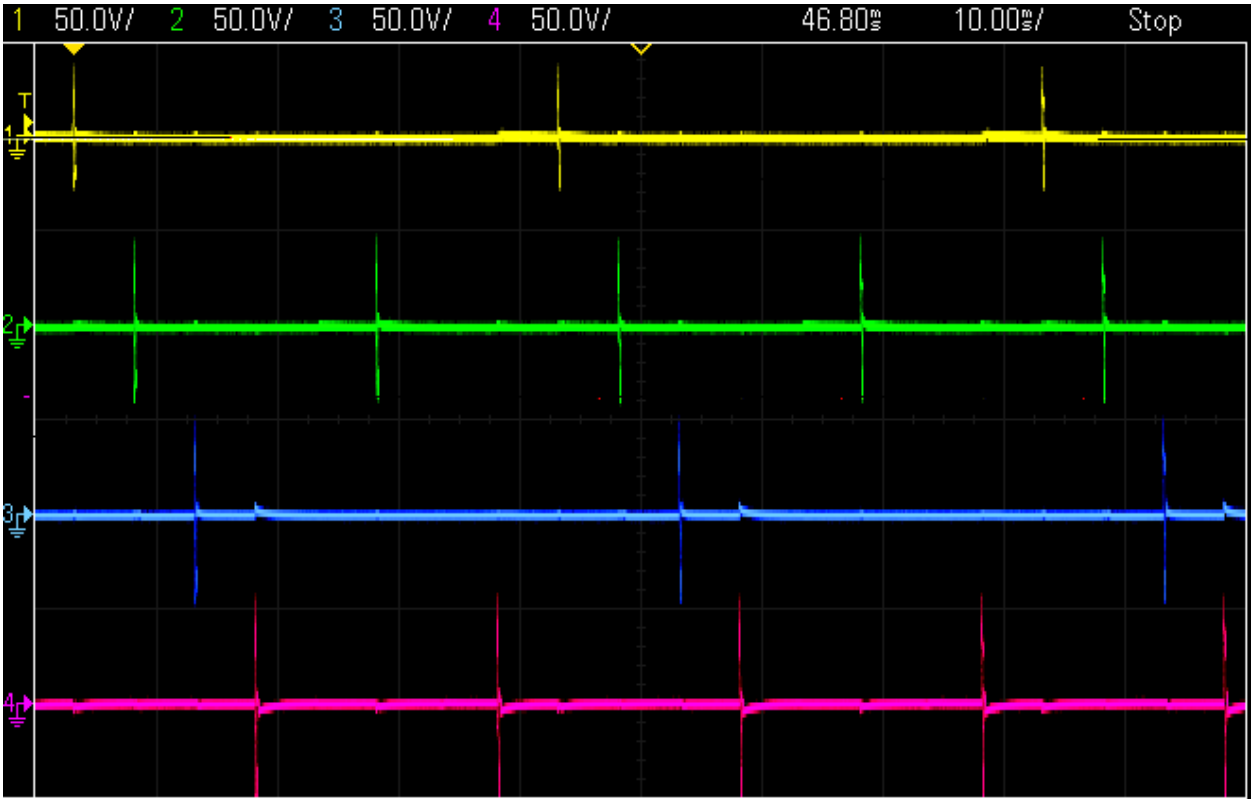

Figure 4.18. Four channels of biphasic pulses generated from a single H-bridge source

CHAPTER V

CONCLUSION

This dissertation presents several control methods for assistive devices designed to provide functional benefits to individuals with mobility impairments. The underlying theme behind each method is maximizing the use of available physiological functions while compensating for the missing portions with sensors and actuators in the robotic device. Whenever deemed appropriate, theoretical principles were employed for the purposes of functionality, and we attempted to simplify each control method as much as possible without compromising functionality. For the volitional control method using EMG presented in Chapter II, a machine learning algorithm was implemented in order to account for variations in EMG signal patterns and baseline noise levels (both between different users and within each user), thus minimizing the need for manual tuning. For the step trigger controller presented in Chapter III, the system was modeled as an inverted pendulum in order to take the user dynamics into account, thus improving the gait speed. For the cooperative controller combining FES with powered lower limb exoskeletons presented in Chapter IV, a step-wise adaptation method was implemented in order to account for variations in muscle response to FES (both between different users and within each user), while providing physiological benefits of using FES. For each control method, utmost priority was given to practicality and usability, so that the proposed method can benefit real people, rather than focus on theoretical aspects for academic purposes.

1. Validation of Efficacy of Control Methods and Statistical Significance

In order to assess the effectiveness of the control methods, each control method was tested on multiple subjects for whom the controller was developed. The volitional control method using EMG was tested on three subjects with transfemoral amputations. The step trigger controller for lower limb exoskeletons was tested on five subjects with motor-complete spinal cord injuries. The cooperative controller combining FES with powered lower limb exoskeletons was tested on

three subjects with motor-complete spinal cord injuries who were FES-responsive. In all cases, results indicate that the proposed control methods are able to provide functional benefits to individuals with mobility impairments.

In addition to providing functional benefits, another important goal of these devices is to provide physiological benefits. However, assessing the extent of physiological benefits would require full-scale clinical trials, which are beyond the scope of this work, as the Center for Intelligent Mechatronics is primarily an engineering laboratory focused on device development. Furthermore, these devices are laboratory prototypes that will undergo significant changes before they become available to end users.

2. Commercial Translation and Conflict of Interest Disclosure

The devices and control methods presented in this dissertation have been licensed to commercial partners. The awarded patents, provisional patent applications, and know-how generated from the powered transfemoral prosthesis have been licensed to Freedom Innovations, LLC, a prosthesis manufacturer based in Irvine, California. I am a co-inventor on a patent licensed to Freedom Innovations, LLC (US Patent 8,623,098 B2, "Systems and method for volitional control of jointed mechanical devices based on surface electromyography," granted, January, 17, 2014), and therefore have a financial interest in the successful commercial translation of the device. The provisional patent applications and know-how generated from the powered lower limb exoskeleton have been licensed to Parker Hannifin Corporation, a multinational manufacturer of motion and control technologies headquartered in Cleveland, Ohio. I am a co-inventor on a provisional patent application and know-how licensed to Parker Hannifin Corporation and therefore have a financial interest in the successful commercial translation of the device.

3. Future Work

It seems to me that there is always more work to be done with any research projects, and that is the case with the work presented in this dissertation. For the volitional control method using EMG presented in Chapter II, one of the downsides of the pattern-recognition controller is that

the controller needs to be trained before use. If there is some form of physiological co-contraction pattern in the residual quadriceps and hamstring muscles while walking using the powered prosthesis, and if there is a correlation between the co-contraction pattern and the user's intent to flex or extend the knee joint, it may be possible to calibrate the controller while walking, so that separate training sessions are not necessary. For the step trigger controller presented in Chapter III, the controller models the system as an inverted pendulum rotating in the sagittal plane (front to back movement), and it does not take the frontal-plane motions into account (side to side movement). This is due to the fact that the current hardware does not have any actuators in the frontal plane. As a result, frontal-plane stability is provided solely by stability aid (i.e. walker or forearm crutches). In the future, implementing frontal-plane actuators (for hip abduction and adduction) could provide frontal-plane stability and reduce dependency on stability aid. For the cooperative controller combining FES with powered exoskeletons presented in Chapter IV, the controller has been shown to be effective for level-ground walking. In the future, the cooperative controller may be implemented for other activities, such as stair ascent and descent,

As for the future direction of the field of assistive robotics in general, it is not obvious how the field will develop over the next decade or two, since the field is still at its infancy. There is still a lot more work to be done in many aspects of the powered prostheses and lower limb exoskeletons. Regardless, in my opinion, one thing we must keep in mind as researchers is that we should take the least invasive course possible for the user. In the case of volitional control of the control of powered prostheses, using surface EMG is likely an acceptable option for most users since the surface electrodes can be embedded in the already existing sockets over the residual limbs, requiring no additional work for the user. For the population with lower limb amputation, anything more invasive seems excessive. Even for individuals with spinal cord injuries, the existing non-invasive methods have been shown to be capable of determining the user's high-level intent (e.g. to walk or to stop walking) with high accuracy. For the purposes of walking, more invasive measures, such as electroencephalography (EEG) or, as an extreme example, cortical electrodes on the user's brain, do not seem that they would ever be an acceptable option. For restoring upper extremity function, the control method will likely require some form of neural connection to the user, which may require more invasive measures for some

users. In the case of using FES along with an exoskeleton, some may be willing to undergo minor surgical procedures to have small wireless stimulators implanted under the skin, since the current method (using wired surface electrodes over the muscles) can be cumbersome and the cost of surface electrodes can add up over time.

In the immediate future, more significant impact (at the user level) will likely come from advancements on the hardware side. The supporting technologies will continue to improve, providing engineers with more accurate sensors, better actuators, and higher capacity batteries. With these advancements, self-contained assistive devices can become smaller, lighter, more powerful, and less expensive, so that they can become widely available and be used by the people who need them.

REFERENCES

[1] E. R. Kandel, "From Nerve Cells to Cognition: The Internal Cellular Representation Required for Perception and Action," in *Principles of Neural Science*, ed, 2000, pp. 381-403.

[2] C. K. Ghez, J., "The Organizatin of Movement," in *Principles of Neural Science*, ed, 2000, pp. 653-673.

[3] R. S. Snell and R. S. Snell. (2006). *Clinical neuroanatomy (6th ed.)*.

[4] C. T. Ghez, W.T., "The Cerebellum," in *Principles of Neural Science*, ed, 2000, pp. 832-852.

[5] K. G. Pearson, J., "Spinal Reflexes," in *Principles of Neural Science*, ed, 2000, pp. 713-736.

[6] G. E. G. Loeb, C., "The Motor Unit and Muscle Action," in *Principles of Neural Science*, ed, 2000, pp. 674-694.

[7] K. T. Ragnarsson, "Functional electrical stimulation after spinal cord injury: current use, therapeutic effects and future directions," *Spinal Cord,* vol. 46, pp. 255-274, Apr 2008.

[8] F. Sup, H. A. Varol, J. Mitchell, T. J. Withrow, and M. Goldfarb, "Preliminary Evaluations of a Self-Contained Anthropomorphic Transfemoral Prosthesis," *IEEE/ASME Transactions on Mechatronics,* vol. 14, pp. 667-676, 2009.

[9] H. A. Varol, F. Sup, and M. Goldfarb, "Multiclass Real-Time Intent Recognition of a Powered Lower Limb Prosthesis," *IEEE Transactions on Biomedical Engineering,* vol. 57, pp. 542-551, 2010.

[10] E. C. Martinez-Villalpando and H. Herr, "Agonist-antagonist active knee prosthesis: a preliminary study in level-ground walking," *J Rehabil Res Dev,* vol. 46, pp. 361-73, 2009.

[11] P. F. Pasquina, P. R. Bryant, M. E. Huang, T. L. Roberts, V. S. Nelson, and K. M. Flood, "Advances in amputee care," *Arch Phys Med Rehabil,* vol. 87, pp. S34-43; quiz S44-5, Mar 2006.

[12] R. R. Torrealba, G. Fernandez-Lopez, and J. C. Grieco, "Towards the development of knee prostheses: review of current researches," *Kybernetes,* vol. 37, pp. 1561-1576, 2008.

[13] D. Popovic and L. Schwirtlich, "Belgrade active A/K prosthesis," *in de Vries, J. (Ed.), Electrophysiological Kinesiology, Intern. Congress Ser. No. 804 Excerpta Medica*, pp. 337-343, 1988.

[14] D. L. Grimes, Flowers, W.C. and Donath, M., "Feasibility of an active control scheme for above knee prostheses," *ASME Journal of Biomechanical Engineering,* vol. 99, pp. 215-221, 1977.

[15] M. Makhsous, M. Priebe, J. Bankard, D. Rowles, M. Zeigler, D. Chen, *et al.*, "Measuring tissue perfusion during pressure relief maneuvers: insights into preventing pressure ulcers," *J Spinal Cord Med,* vol. 30, pp. 497-507, 2007.

[16] G. Horn, "Electro-control: am EMG-controlled A/K prosthesis," *Medical and Biological Engineering and Computing,* vol. 10, pp. 61-73, 1972.

[17] S. C. Saxena and P. Mukhopadhyay, "Emg Operated Electronic Artificial-Leg Controller," *Medical & Biological Engineering & Computing,* vol. 15, pp. 553-557, 1977.

[18] L. Peeraer, B. Aeyels, and G. Van der Perre, "Development of EMG-based mode and intent recognition algorithms for a computer-controlled above-knee prosthesis," *J Biomed Eng,* vol. 12, pp. 178-82, May 1990.

[19] B. Aeyels, L. Peeraer, J. Vander Sloten, and G. Van der Perre, "Development of an above-knee prosthesis equipped with a microcomputer-controlled knee joint: first test results," *J Biomed Eng,* vol. 14, pp. 199-202, May 1992.

[20] B. Aeyels, W. Van Petegem, J. V. Sloten, G. Van Der Perre, and L. Peeraer, "An EMG-based finite state approach for a microcomputer-controlled above-knee prosthesis," in *IEEE 17th Annual Conference of Engineering in Medicine and Biology Society*, 1995, pp. 1315-1316 vol.2.

[21] H. Huang, T. A. Kuiken, and R. D. Lipschutz, "A Strategy for Identifying Locomotion Modes Using Surface Electromyography," *IEEE Transactions on Biomedical Engineering,* vol. 56, pp. 65-73, Jan 2009.

[22] H. Huang, P. Zhou, G. Li, and T. A. Kuiken, "An Analysis of EMG Electrode Configuration for Targeted Muscle Reinnervation Based Neural Machine Interface," *Neural Systems and Rehabilitation Engineering, IEEE Transactions on,* vol. 16, pp. 37-45, 2008.
[23] M. Donath, "Proportional EMG control for above-knee prosthesis," *Master's Thesis, Cambridge, MA, MIT, Department of Mechanical Engineering,* 1974.
[24] S. K. Au, P. Bonato, and H. Herr, "An EMG-position controlled system for an active ankle-foot prosthesis: an initial experimental study," in *9th International Conference on Rehabilitation Robotics*, 2005, pp. 375-379.
[25] S. Au, M. Berniker, and H. Herr, "Powered ankle-foot prosthesis to assist level-ground and stair-descent gaits," *Neural Netw,* vol. 21, pp. 654-66, May 2008.
[26] D. P. Ferris, J. M. Czerniecki, and B. Hannaford, "An ankle-foot orthosis powered by artificial pneumatic muscles," *J Appl Biomech,* vol. 21, pp. 189-97, May 2005.
[27] D. P. Ferris, K. E. Gordon, G. S. Sawicki, and A. Peethambaran, "An improved powered ankle-foot orthosis using proportional myoelectric control," *Gait Posture,* vol. 23, pp. 425-8, Jun 2006.
[28] S. M. Cain, K. E. Gordon, and D. P. Ferris, "Locomotor adaptation to a powered ankle-foot orthosis depends on control method," *J Neuroeng Rehabil,* vol. 4, p. 48, 2007.
[29] H. Kawamoto and Y. Sankai, "Power Assist System HAL-3 for Gait Disorder Person," in *Computers Helping People with Special Needs*, ed, 2002, pp. 19-29.
[30] G. J. McLachlan, W. John, Sons, and I. Wiley, *Discriminant analysis and statistical pattern recognition*. Hoboken, N.J.: Wiley-Interscience, 2004.
[31] I. T. Jolliffe, *Principal Component Analysis*: Springer, 2002.
[32] D. L. Brown-Triolo, M. J. Roach, K. Nelson, and R. J. Triolo, "Consumer perspectives on mobility: implications for neuroprosthesis design," *J Rehabil Res Dev,* vol. 39, pp. 659-69, Nov-Dec 2002.
[33] E. J. Nightingale, J. Raymond, J. W. Middleton, J. Crosbie, and G. M. Davis, "Benefits of FES gait in a spinal cord injured population," *Spinal Cord,* vol. 45, pp. 646-57, Oct 2007.
[34] S. C. Chen, C. H. Lai, W. P. Chan, M. H. Huang, H. W. Tsai, and J. J. Chen, "Increases in bone mineral density after functional electrical stimulation cycling exercises in spinal cord injured patients," *Disabil Rehabil,* vol. 27, pp. 1337-41, Nov 30 2005.
[35] P. Krause, J. Szecsi, and A. Straube, "Changes in spastic muscle tone increase in patients with spinal cord injury using functional electrical stimulation and passive leg movements," *Clinical Rehabilitation,* vol. 22, pp. 627-634, Jul 2008.
[36] M. Belanger, R. B. Stein, G. D. Wheeler, T. Gordon, and B. Leduc, "Electrical stimulation: Can it increase muscle strength and reverse osteopenia in spinal cord injured individuals?," *Archives of Physical Medicine and Rehabilitation,* vol. 81, pp. 1090-1098, Aug 2000.
[37] P. H. Peckham and J. S. Knutson, "Functional electrical stimulation for neuromuscular applications," *Annual Review of Biomedical Engineering,* vol. 7, pp. 327-360, 2005.
[38] H. P. a. P. H. Gorman, "Functional Electrical Stimulation in the 21st Century," *Topics in Spinal Cord Injury Rehabilitation,* vol. 10, pp. 126-150, 2004.
[39] K. Suzuki, G. Mito, H. Kawamoto, Y. Hasegawa, and Y. Sankai, "Intention-based walking support for paraplegia patients with Robot Suit HAL," *Advanced Robotics,* vol. 21, pp. 1441-1469, Dec 2007.
[40] A. M. Dollar and H. Herr, "Lower extremity exoskeletons and active orthoses: Challenges and state-of-the-art," *Ieee Transactions on Robotics,* vol. 24, pp. 144-158, Feb 2008.
[41] Y. Hasegawa, J. Junho, and Y. Sankai, "Cooperative walk control of paraplegia patient and assistive system," in *Intelligent Robots and Systems, 2009. IROS 2009. IEEE/RSJ International Conference on*, 2009, pp. 4481-4486.
[42] A. Tsukahara, Y. Hasegawa, and Y. Sankai, "Standing-up motion support for paraplegic patient with Robot Suit HAL," in *Rehabilitation Robotics, 2009. ICORR 2009. IEEE International Conference on*, 2009, pp. 211-217.

[43] K. Hian Kai, J. H. Noorden, M. Missel, T. Craig, J. E. Pratt, and P. D. Neuhaus, "Development of the IHMC Mobility Assist Exoskeleton," in *Robotics and Automation, 2009. ICRA '09. IEEE International Conference on*, 2009, pp. 2556-2562.

[44] A. Tsukahara, R. Kawanishi, Y. Hasegawa, and Y. Sankai, "Sit-to-Stand and Stand-to-Sit Transfer Support for Complete Paraplegic Patients with Robot Suit HAL," *Advanced Robotics*, vol. 24, pp. 1615-1638, 2010.

[45] P. D. Neuhaus, J. H. Noorden, T. J. Craig, T. Torres, J. Kirschbaum, and J. E. Pratt, "Design and evaluation of Mina: A robotic orthosis for paraplegics," in *Rehabilitation Robotics (ICORR), 2011 IEEE International Conference on*, 2011, pp. 1-8.

[46] R. J. Farris, H. A. Quintero, and M. Goldfarb, "Preliminary evaluation of a powered lower limb orthosis to aid walking in paraplegic individuals," *IEEE Trans Neural Syst Rehabil Eng,* vol. 19, pp. 652-9, Dec 2011.

[47] H. A. Quintero, R. J. Farris, and M. Goldfarb, "A Method for the Autonomous Control of Lower Limb Exo-skeletons for Persons with Paraplegia," *J Med Device,* vol. 6, Dec 12 2012.

[48] Y. Ohta, H. Yano, R. Suzuki, M. Yoshida, N. Kawashima, and K. Nakazawa, "A two-degree-of-freedom motor-powered gait orthosis for spinal cord injury patients," *Proceedings of the Institution of Mechanical Engineers Part H-Journal of Engineering in Medicine,* vol. 221, pp. 629-639, Aug 2007.

[49] A. Esquenazi, M. Talaty, A. Packel, and M. Saulino, "The ReWalk powered exoskeleton to restore ambulatory function to individuals with thoracic-level motor-complete spinal cord injury," *Am J Phys Med Rehabil,* vol. 91, pp. 911-21, Nov 2012.

[50] R. Farris, H. Quintero, S. Murray, K. Ha, C. Hartigan, and M. Goldfarb, "A Preliminary Assessment of Legged Mobility provided by a Lower Limb Exoskeleton for Persons with Paraplegia," *IEEE Trans Neural Syst Rehabil Eng,* Jun 18 2013.

[51] A. W. Andrews, S. A. Chinworth, M. Bourassa, M. Garvin, D. Benton, and S. Tanner, "Update on distance and velocity requirements for community ambulation," *J Geriatr Phys Ther,* vol. 33, pp. 128-34, Jul-Sep 2010.

[52] J. Perry, M. Garrett, J. K. Gronley, and S. J. Mulroy, "Classification of walking handicap in the stroke population," *Stroke,* vol. 26, pp. 982-9, Jun 1995.

[53] R. J. Farris, H. A. Quintero, and M. Goldfarb, "Preliminary Evaluation of a Powered Lower Limb Orthosis to Aid Walking in Paraplegic Individuals," *Neural Systems and Rehabilitation Engineering, IEEE Transactions on,* vol. 19, pp. 652-659, 2011.

[54] P. Rossier and D. T. Wade, "Validity and reliability comparison of 4 mobility measures in patients presenting with neurologic impairment," *Arch Phys Med Rehabil,* vol. 82, pp. 9-13, Jan 2001.

[55] M. Schenkman, T. M. Cutson, M. Kuchibhatla, J. Chandler, and C. Pieper, "Reliability of impairment and physical performance measures for persons with Parkinson's disease," *Phys Ther,* vol. 77, pp. 19-27, Jan 1997.

[56] M. T. Smith and G. D. Baer, "Achievement of simple mobility milestones after stroke," *Arch Phys Med Rehabil,* vol. 80, pp. 442-7, Apr 1999.

[57] H. J. van Hedel, M. Wirz, and V. Dietz, "Assessing walking ability in subjects with spinal cord injury: validity and reliability of 3 walking tests," *Arch Phys Med Rehabil,* vol. 86, pp. 190-6, Feb 2005.

[58] M. O. L. Phillips, P. Axelson, and J. Fonseca, *Spinal cord injury: A guide for patient and family*: Raven Press, 1987.

[59] A. Kralj, T. Bajd, R. Turk, J. Krajnik, and H. Benko, "Gait restoration in paraplegic patients: a feasibility demonstration using multichannel surface electrode FES," *Journal of rehabilitation R&D / Veterans Administration, Department of Medicine and Surgery, Rehabilitation R&D Service,* vol. 20, pp. 3-20, 1983.

[60] E. B. Marsolais and R. Kobetic, "Functional walking in paralyzed patients by means of electrical stimulation," *Clin Orthop Relat Res*, pp. 30-6, May 1983.
[61] G. R. Cybulski, R. D. Penn, and R. J. Jaeger, "Lower extremity functional neuromuscular stimulation in cases of spinal cord injury," *Neurosurgery*, vol. 15, pp. 132-46, Jul 1984.
[62] A. R. Kralj and T. Bajd, *Functional electrical stimulation: standing and walking after spinal cord injury*: CRC Press, 1989.
[63] P. Gallien, R. Brissot, M. Eyssette, L. Tell, M. Barat, L. Wiart, *et al.*, "Restoration of gait by functional electrical stimulation for spinal cord injured patients," *Paraplegia*, vol. 33, pp. 660-4, Nov 1995.
[64] R. Dai, R. B. Stein, B. J. Andrews, K. B. James, and M. Wieler, "Application of tilt sensors in functional electrical stimulation," *Rehabilitation Engineering, IEEE Transactions on*, vol. 4, pp. 63-72, 1996.
[65] R. Kobetic, R. J. Triolo, and E. B. Marsolais, "Muscle selection and walking performance of multichannel FES systems for ambulation in paraplegia," *IEEE Trans Rehabil Eng*, vol. 5, pp. 23-9, Mar 1997.
[66] D. Graupe and K. H. Kohn, "Functional neuromuscular stimulator for short-distance ambulation by certain thoracic-level spinal-cord-injured paraplegics," *Surg Neurol*, vol. 50, pp. 202-7, Sep 1998.
[67] M. M. Skelly and H. J. Chizeck, "Real-time gait event detection for paraplegic FES walking," *Neural Systems and Rehabilitation Engineering, IEEE Transactions on*, vol. 9, pp. 59-68, 2001.
[68] X. Zhaojun, W. Dahai, M. Dong, and W. Baikun, "New Gait Recognition Technique Used in Functional Electrical Stimulation System Control," in *Intelligent Control and Automation, 2006. WCICA 2006. The Sixth World Congress on*, 2006, pp. 9421-9424.
[69] A. Dutta, R. Kobetic, and R. Triolo, "Walking after partial paralysis assisted with EMG-triggered or switch-triggered functional electrical stimulation — Two case studies," in *Rehabilitation Robotics (ICORR), 2011 IEEE International Conference on*, 2011, pp. 1-6.
[70] D. Popovic, R. Tomovic, and L. Schwirtlich, "Hybrid assistive system--the motor neuroprosthesis," *IEEE Trans Biomed Eng*, vol. 36, pp. 729-37, Jul 1989.
[71] M. Solomonow, R. Baratta, S. Hirokawa, N. Rightor, W. Walker, P. Beaudette, *et al.*, "The RGO Generation II: muscle stimulation powered orthosis as a practical walking system for thoracic paraplegics," *Orthopedics*, vol. 12, pp. 1309-15, Oct 1989.
[72] M. Goldfarb, K. Korkowski, B. Harrold, and W. Durfee, "Preliminary evaluation of a controlled-brake orthosis for FES-aided gait," *IEEE Trans Neural Syst Rehabil Eng*, vol. 11, pp. 241-8, Sep 2003.
[73] W. K. Durfee and A. Rivard, "Design and simulation of a pneumatic, stored-energy, hybrid orthosis for gait restoration," *J Biomech Eng*, vol. 127, pp. 1014-9, Nov 2005.
[74] C. S. To, R. Kobetic, J. R. Schnellenberger, M. L. Audu, and R. J. Triolo, "Design of a variable constraint hip mechanism for a hybrid neuroprosthesis to restore gait after spinal cord injury," *Ieee-Asme Transactions on Mechatronics*, vol. 13, pp. 197-205, Apr 2008.
[75] R. Kobetic, C. S. To, J. R. Schnellenberger, M. L. Audu, T. C. Bulea, R. Gaudio, *et al.*, "Development of hybrid orthosis for standing, walking, and stair climbing after spinal cord injury," *Journal of Rehabilitation Research and Development*, vol. 46, pp. 447-462, 2009.
[76] M. L. Audu, C. S. To, R. Kobetic, and R. J. Triolo, "Gait Evaluation of a Novel Hip Constraint Orthosis With Implication for Walking in Paraplegia," *Ieee Transactions on Neural Systems and Rehabilitation Engineering*, vol. 18, pp. 610-618, Dec 2010.
[77] A. J. del-Ama, A. D. Koutsou, J. C. Moreno, A. de-los-Reyes, A. Gil-Agudo, and J. L. Pons, "Review of hybrid exoskeletons to restore gait following spinal cord injury," *Journal of Rehabilitation Research and Development*, vol. 49, pp. 497-514, 2012.
[78] Rewalk. *Argo Medical Technologies*. Available: http://www.rewalk.com/
[79] Ekso. *Ekso Bionics*. Available: http://www.eksobionics.com/

[80] G. Obinata, S. Fukada, T. Matsunaga, T. Iwami, Y. Shimada, K. Miyawaki, *et al.*, "Hybrid control of powered orthosis and functional neuromuscular stimulation for restoring gait," *Conf Proc IEEE Eng Med Biol Soc*, vol. 2007, pp. 4879-82, 2007.
[81] A. J. del-Ama, A. Gil-Agudo, J. L. Pons, and J. C. Moreno, "Hybrid FES-robot cooperative control of ambulatory gait rehabilitation exoskeleton," *J Neuroeng Rehabil*, vol. 11, p. 27, 2014.
[82] K. L. Moore, A. F. Dalley, and A. M. R. Agur, *Clinically oriented anatomy*, 6th ed. Philadelphia: Wolters Kluwer/Lippincott Williams & Wilkins, 2010.